

Fundamentals of High Energy X-ray and Electron Dosimetry Protocols

David W.O. Rogers

Current address: Physics Department, Carleton University
Ottawa K1S 5B6, Canada
drogers at physics dot carleton dot ca

This is a slightly modified version of a chapter presented at the 1990 AAPM Summer School and published in AAPM Monograph 19, Advances in Radiation Oncology Physics, edited by J. Purdy, pages 181-223, 1992, AAPM, New York. The figures are redrawn with current software from the original data and the table of contents has been moved forward. The original pagination is retained

Contents

1	Introduction.	181
2	TG-21: Its successes and its problems.	182
3	Proposed Resolution of the Problems.	182
4	The TG-21 Protocol.	182
4.1	Fundamentals and Notation.	183
4.1.1	Particle Fluence.	183
4.1.2	Collision Kerma.	184
4.1.3	$(W/e)_{\text{air}}$	184
4.1.4	Exposure and Air Kerma.	185
4.1.5	Charged Particle Equilibrium, Dose and Collision Kerma.	185
4.1.6	Particle Fluence and Dose.	186
4.1.7	Bragg-Gray Cavity Theory.	186
4.1.8	Spencer-Attix Cavity Theory.	187
4.1.9	Charge Measurement.	188
4.1.10	Exposure and Air Kerma Calibration Factors.	189
4.2	Exposure and Ion Chamber Response.	189
4.2.1	Derivation of the Basic Equation.	189
4.2.2	Humidity Correction Factor.	190
4.2.3	The Other Correction Factors: $K_{\text{wall}}, K_{\text{an}}, K_{\text{st}}, K_{\text{el}}, K_{\text{comp}}$	191
4.3	N_{gas} – The Cavity-Gas Calibration Factor.	193
4.3.1	Definition of N_{gas}	193
4.3.2	Derivation of the Expression for N_{gas}	193
4.3.3	N_{gas} in Terms of the Air Kerma Calibration Factor.	195

4.3.4	N_{gas} Compared to AAPM Values.	195
4.3.5	Translation to AAPM TG-21 Notation.	196
4.3.6	Evaluation of K_{comp}	196
4.3.7	α Values in a ^{60}Co beam.	197
4.3.8	Values of N_{gas}	197
4.4	The Dose to the Medium.	198
4.4.1	General Considerations.	198
4.4.2	P_{ion} Corrections for Charge Collection.	199
4.4.3	P_{wall} Correction Factors.	200
4.4.4	A Conceptual Problem with P_{wall} and K_{comp}	202
4.4.5	Specifying Photon Beam Quality – NAP.	203
4.4.6	Specifying Electron Beam Quality – \bar{E}_0	204
4.4.7	The Replacement Correction Factor, $P_{\text{repl}} = P_{\text{gr}}P_{\text{fl}}$	205
4.4.8	Use of Plastic Phantoms.	209
4.5	Exact Treatment of Humidity Effects.	210
4.6	Stopping Power Inconsistencies.	210
5	The IAEA Code of Practice	211
5.1	Fundamentals of the IAEA Code of Practice.	211
5.2	Phantom Material.	212
5.3	Beam Quality and Average Energy Specification.	212
5.3.1	Electrons.	212
5.3.2	Photons.	212
5.4	IAEA Formalism.	213
5.5	IAEA Equation for the Dose to the Medium.	213
6	Acknowledgements.	214
7	Appendices.	215
7.1	A: Proof of Fluence and Dose Equation.	215
7.2	B: Derivations of K_{comp} and P_{wall}	216
7.3	Appendix C	218
8	References.	220

Fundamentals of High Energy X-ray and Electron Dosimetry Protocols ¹

David W.O. Rogers

Institute for National Measurement Standards
National Research Council of Canada, Ottawa, K1A 0R6, Canada

Abstract

Using a consistent notation and starting from basic principles, the physical concepts involved in clinical dosimetry protocols are reviewed and derivations are given of the fundamental equations of both the TG-21 protocol and the IAEA Code of Practice. While emphasizing that the TG-21 protocol gives accurate dose estimates, attention is drawn to the following problems in TG-21: the equation for N_{gas} is incorrect; the equation for K_{comp} is not that given in the referenced paper although it gives the same results; the physical data used are inconsistent, in particular the stopping-power ratios for photon beams; the accuracy of the P_{wall} correction factor is not well established and needs to account for a water-proofing sleeve; the photon beam gradient correction factors are considerably different from the data on which the IAEA bases its equivalent correction (1.3% vs 0.9% for a Farmer chamber in ^{60}Co beams). A complete table of contents is found in an Appendix.

1 Introduction.

The purpose of dosimetry protocols is to determine, under a specified set of reference conditions, the absorbed dose to water delivered by accelerator or ^{60}Co beams incident on a water phantom. This is a very restricted objective since clinical physicists really need to know the dose at many locations in a patient. However, even the limited objective of the protocols is a complex topic.

Most current protocols recommend using ion chambers as the measuring instrument and start from the exposure or air kerma calibration factors (which are related by a simple numerical factor). These chambers are used as cavity chambers in a phantom and Spencer-Attix cavity theory is applied to determine the absorbed dose. The resulting procedure depends explicitly on the characteristics of the ion chamber used. This approach is in contrast to the previous one recommended by ICRU-14 in which the ion chamber was thought of as measuring the exposure in the hole it created in the phantom when irradiated by a ^{60}Co beam. Absorbed doses in higher energy beams were determined using corrections based on Bragg-Gray cavity theory. This procedure contained no chamber dependence other than the calibration factor and had errors of up to 3 to 5%. This led to a vast literature in the 70's as things were sorted out.

By the late 70's, both the AAPM and NACP were converging towards a new approach (see, for example the discussion after the paper by Johansson *et al.*, 1977).

¹In original, table of contents was an appendix

The resulting protocols (AAPM, 1983 and NACP, 1980) share many similarities in overall approach and data although the formalisms look somewhat different. In essence, both use an exposure calibration to determine the mass of the gas in the ion chamber and then apply Spencer-Attix cavity theory, with corrections, to determine the dose in the phantom.

2 TG-21: Its successes and its problems.

The major successes of the AAPM protocol are that it presented an excellent framework for analysing the various factors involved in determining absorbed dose using exposure calibrated ion chambers and it still gives values which are within 1% or so of the current best estimates. This is important to keep in mind as this chapter is read, and many errors and uncertainties in the protocol are discussed. Since the net effect of all the changes appears to average to zero, **one should still use the original protocol as it is written.** This ensures proper documentation and leads to the best available consistency in dose assignments at various centers and using different modalities.

On the other side of the coin, the protocol has many problems. The most serious is that it is very complex to apply. Further, because of many mistakes both in the logic of the derivations and in the inconsistent use of data, it is very hard to understand. This means mistakes are possible. A framework which is useful for research is more powerful than needed in a clinic.

The final problem is that the inherent accuracy of the AAPM protocol and all similar protocols is only ± 3 to 4%. The fact that various protocols all give the same result to within about 1% implies nothing about the overall accuracy because they all use basically the same data and approach.

3 Proposed Resolution of the Problems.

The inherent complexity of the protocol is hard to overcome but a rigorous and coherent derivation of the main equations will be presented here. The problems of the mistakes and inconsistent use of data in the protocol have been, to a large extent, overcome in the IAEA Code of Practice which is discussed in some detail in section 5. It has the same basic approach as the AAPM protocol (two AAPM TG-21 members helped to write it) but still faces some of the same underlying uncertainties.

As discussed in my other chapter on “New Dosimetry Standards”, the best way to resolve the problems and improve the uncertainty in the assigned dose may be to use an entirely new approach based on absorbed dose standards and calibration factors.

4 The TG-21 Protocol.

This section derives the equations and defines the quantities which appear in the TG-21 protocol using a consistent notation since one of the great problems with the TG-21 protocol is sloppy use of notation. It will also review the status of various factors used in the protocol.

The approach used is consistent with the intent of the TG-21 protocol but is different. The actual presentation is a simplification of a paper by Carl Ross and myself (1988, referred to as RR88 hereafter). The fundamental approach to the use of correction factors for in-air ion chambers is based on the work of my colleague Alex Bielajew who has presented a rigorous formalism which shows how to calculate these factors using Monte-Carlo techniques (Bielajew, 1986, 1990a).

Use of a consistent set of quantities and units greatly clarifies the meaning of various relationships. Thus only SI units are used. This eliminates the need of the AAPM's k factor of 2.58×10^{-4} (C/kg)/R since exposure is always in C/kg rather than R.

4.1 Fundamentals and Notation.

In this section, a series of definitions and fundamental relationships will be given to establish notation and ensure a common starting point. More detailed discussions can be found in Attix's text (1986) and in various ICRU reports. As a convenience, the term electron will be taken to include electrons and positrons.

4.1.1 Particle Fluence.

The ICRU defines particle fluence, Φ as the quotient of dN by da , where dN is the number of particles incident on a **sphere** of cross-sectional area da .

$$\Phi = \frac{dN}{da} \quad (\text{m}^{-2}). \quad (1)$$

Care must be taken to distinguish fluence from planar fluence which is the number of particles crossing a plane per unit area. In figure 1 the **particle fluence** is the

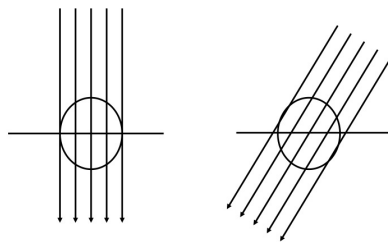


Figure 1: The particle fluence is the same in both cases.

same in both cases because the number of particles hitting the sphere is the same whereas the **planar fluence** *decreases* when the beam is not at normal incidence.

An alternative definition of particle fluence is that it is equal to the sum of the particle track lengths in a volume, divided by the volume. This formulation is equivalent to the formal definition (see Chilton, 1978 and 1979) and means:

$$\Phi = \frac{\Sigma(\text{tracklengths in volume})}{\text{volume}}. \quad (2)$$

4.1.2 Collision Kerma.

Collision kerma is the kinetic energy per unit mass transferred to electrons by a photon beam and not subsequently lost by radiative processes (i.e. it is the amount of energy dissipated “locally” by ionization). It is a point function given by:

$$(K_c)_{\text{med}} = E_\gamma \phi_\gamma \left(\frac{\overline{\mu_{\text{en}}}}{\rho} \right)_{\text{med}} \quad (\text{J/kg}), \quad (3)$$

where E_γ is the average energy of the photons (J); ϕ_γ is the photon fluence (m^{-2}) at the point and $(\overline{\mu_{\text{en}}}/\rho)_{\text{med}}$ is the mass-energy absorption coefficient for the medium averaged over the energy fluence spectrum of photons (m^2/kg). See Attix (1979) for a more complete discussion of this useful concept.

A more general quantity is the kerma which is the kinetic energy per unit mass transferred to electrons by a photon beam. It is related to the collision kerma by:

$$(K_c)_{\text{med}} = K_{\text{med}}(1 - \bar{g}) \quad (\text{J/kg}), \quad (4)$$

where \bar{g} is the average fraction of an electron’s energy lost via radiative processes. Table 1 gives the currently recommended values of \bar{g} .

Table 1:

Values of \bar{g} for electrons generated in air by photon beams of various qualities as recommended by the CCEMRI, (1985) based on calculations by Boutillon using the electron stopping-powers in ICRU Report 37.

Beam Quality	\bar{g}
< 50 kV	< 0.0001
100 – 135 kV	0.0001
180 kV	0.00016
250 kV	0.00028
^{60}Co	0.0032

4.1.3 $(W/e)_{\text{air}}$.

As an electron slows down in a gas, it loses energy by ionizing the gas. The quantity \overline{W} is the mean energy expended in the gas per ion pair formed, usually expressed in units of eV per ion pair.

For dry air, this quantity is found to be a constant, independent of the electron energy above a few keV. A more useful form of this quantity is in terms of the charge released. Dividing by the charge of the electron, gives $(W/e)_{\text{air}} = 33.97 \pm 0.06$ (J/C). $(W/e)_{\text{air}}$ gives the joules of energy deposited in air per coulomb of charge released. Alternatively, $(e/W)_{\text{air}}$ gives the coulombs of charge released per joule of energy deposited in air.

Two classes of experiments are used to determine $(W/e)_{\text{air}}$. One class compares the calorimetric and ionometric measurements of absorbed dose in a phantom

(usually carbon) and the second compares the activity of a source and the exposure at some distance from it. Both classes of experiments measure the product $\left(\frac{W}{e}\right)_{\text{air}} \left(\bar{L}/\rho\right)_{\text{air}}^{\text{med}}$ where $\left(\bar{L}/\rho\right)_{\text{air}}^{\text{med}}$ is the stopping-power ratio as defined in section 4.1.8. The 1984 changes in recommended electron stopping powers (ICRU Report 37) means that there has been a change in the accepted value of $(W/e)_{\text{air}}$. The old value, whose determination is discussed at length in ICRU Report 31 (1979), was $33.85 \pm 0.05 \text{ J C}^{-1}$. Based on two more recent experiments (Niatel *et al*, 1985) and on a re-evaluation of all previous data (Boutillon and Perroche-Roux, 1987), in 1985 the BIPM recommended a value of $33.97 \pm 0.06 \text{ J C}^{-1}$ which is consistent with the ICRU Report 37 stopping powers.

Note that all of the above values refer to **dry** air. The ratio of (W/e) values in humid vs dry air has been determined several times (see ICRU Report 31 and references therein). It is plotted vs relative humidity below in fig 3. The AAPM protocol used a ratio $(W/e)_{\text{air}}^{50\%} = 0.994$ (rather than 0.9933) and thus recommended values for $(W/e)_{50\%}$ of 33.7 ($=33.85 \times 0.994$) in 1983 and 33.77 ($=33.97 \times 0.994$) in 1986 (although, as will be seen later, one actually needs $(W/e)_{\text{air}}$).

4.1.4 Exposure and Air Kerma.

Exposure, X , is defined by the ICRU as the quotient of dQ by dm where the value of dQ is the absolute value of the total charge of the ions of one sign produced in (dry) air when all the electrons liberated by photons in air of mass dm are completely stopped in air, i.e.:

$$X = \frac{dQ}{dm} \quad (\text{C/kg}), \quad (5)$$

Exposure is the ionization equivalent of the collision kerma in air for photons. To see this, recall that collision kerma is defined as the energy transferred (less radiative losses) to charged particles per unit mass. Multiplying by $(e/W)_{\text{air}}$, the number of coulombs of charge created per joule of energy deposited gives the charge created per unit mass of air, i.e. the exposure:

$$X = (K_c)_{\text{air}} \left(\frac{e}{W}\right)_{\text{air}} \quad (\text{C/kg}), \quad (6)$$

$$= E_\gamma \phi_\gamma \left(\frac{\mu_{\text{en}}}{\rho}\right)_{\text{air}} \left(\frac{e}{W}\right)_{\text{air}}. \quad (7)$$

This latter eqn gives a method to calculate the exposure at a point knowing the photon fluence there. Using the relationship between kerma and collision kerma (eqn 4) leads to:

$$K_{\text{air}} = X \left(\frac{W}{e}\right)_{\text{air}} / (1 - \bar{g}) \quad (\text{Gy}) \quad (8)$$

4.1.5 Charged Particle Equilibrium, Dose and Collision Kerma.

Charged particle equilibrium (CPE) exists for a volume, v , if each charged particle of a given type and energy leaving v is replaced by an identical particle entering. One implication of this definition is that CPE can only hold if there is no photon

attenuation in a medium. When CPE exists:

$$D_{med} \stackrel{CPE}{=} (K_c)_{med} = \Psi \left(\frac{\overline{\mu_{en}}}{\rho} \right)_{med} \quad (\text{Gy}), \quad (9)$$

i.e. under conditions of CPE at a point in a medium, the absorbed dose is equal to the collision kerma there. This is true irrespective of radiative losses. This is a non-trivial result for which Attix (1986, p 69) gives a good derivation.

Under conditions of charged particle equilibrium, based on the previous results, a very useful relationship can be seen to hold for the absorbed doses in two different media which are in the same photon fluence:

$$\frac{D_A}{D_B} \stackrel{CPE}{=} \frac{(K_c)_A}{(K_c)_B} = \frac{\left(\frac{\overline{\mu_{en}}}{\rho} \right)_A}{\left(\frac{\overline{\mu_{en}}}{\rho} \right)_B} = \left(\frac{\overline{\mu_{en}}}{\rho} \right)_B^A \quad (10)$$

where the last equality only defines the notation.

In photon beams, even past the buildup region, CPE does not occur because of the attenuation and scatter of the beam. In these situations, a case of transient charged particle equilibrium is said to hold if there is lateral equilibrium, because it is found that the shapes of the electron spectra do not vary significantly with depth. In this case, eqn 10 still holds, at least for materials which are not too dissimilar.

4.1.6 Particle Fluence and Dose.

If one assumes that radiative photons escape from the volume of interest and secondary electrons are absorbed on the spot, an important relationship between absorbed dose and the fluence of primary electrons is:

$$D = \Phi(S/\rho)_{col} \quad (\text{Gy}). \quad (11)$$

where $(S/\rho)_{col}$ is the unrestricted collision stopping power. A proof of this important result is given in Appendix A. The assumption that electrons are absorbed on the spot doesn't hold, but for conditions of **charged particle equilibrium of secondary electrons**, the result is still valid because energy transported out of the volume by knock-on electrons is replaced by similar ones coming in.

So far, the fluence has been for mono-energetic electrons. For an electron spectrum up to energy T_{max} we define the spectrum-averaged collision stopping power as:

$$\left(\frac{\overline{S}}{\rho} \right) = \frac{\int_0^{T_{max}} \Phi_T(S/\rho)_{col} dT}{\int_0^{T_{max}} \Phi_T dT} = \frac{D}{\Phi}, \quad (12)$$

where $\Phi_T dT$ is the fluence of particles with energies between T and $T+dT$. Note that these equations make use of the unrestricted collision stopping powers. The effects of knock-on electrons are included in these stopping powers. Thus one integrates over the fluence spectra for **primary** electrons only.

4.1.7 Bragg-Gray Cavity Theory.

Consider a region of otherwise homogeneous medium w which contains a thin layer, or cavity filled with another medium g.

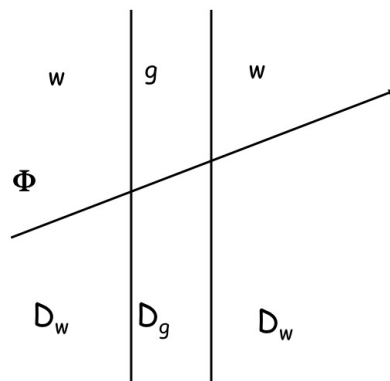


Figure 2: Charged particles of fluence Φ crossing a thin layer of material g in an otherwise uniform medium w (after Attix, 1986)

Bragg-Gray Conditions

- The thickness of the g -layer is assumed to be so small in comparison with the range of charged particles striking it that its presence does not perturb the charged-particle field,
- The absorbed dose in the cavity is assumed to be deposited entirely by the charged particles crossing it (as opposed to being created in it).

The latter condition is valid for gas-filled cavities in photon beams.

When the two Bragg-Gray (B-G) conditions hold, since Φ does not change, eqn 12 gives a ratio of the dose to medium w to that in medium g :

$$\frac{D_w}{D_g} = \frac{\left(\frac{\bar{S}}{\rho}\right)_w}{\left(\frac{\bar{S}}{\rho}\right)_g} = \left(\frac{\bar{S}}{\rho}\right)_g^w \quad (13)$$

where the unrestricted collision stopping power is averaged over the spectrum of **primary** electrons.

Recall that the theory requires CPE of at least the knock-on electrons to use the relationship between dose, fluence and stopping powers. If there is also CPE or transient CPE for the primary electron spectrum (as in a photon beam) certain computational shortcuts are possible.

4.1.8 Spencer-Attix Cavity Theory.

Spencer and Attix (1955) showed that one needs to consider the effects of secondary electrons in cavity theory. The modern formulation of their theory leads to a ratio of the doses in medium w and g given by:

$$\frac{D_m}{D_g} = \left(\frac{\bar{L}}{\rho}\right)_g^m = \frac{\int_{\Delta}^{E_{max}} \Phi_T \left(\frac{L(\Delta)}{\rho}\right)_m dE + TE_m}{\int_{\Delta}^{E_{max}} \Phi_T \left(\frac{L(\Delta)}{\rho}\right)_g dE + TE_g} \quad (14)$$

where TE is a term to account for the 5 to 10% of the dose from track-ends (i.e. electrons whose energy falls below Δ), and Δ is the lowest energy for which secondary electrons are considered part of the electron spectrum (all secondaries below this are considered as absorbed on the spot and included in the restricted stopping power (L/ρ)). There are only small differences between Spencer-Attix and Bragg-Gray cavity theory results for most situations of interest in clinical physics. The advantage of Spencer-Attix theory is that it applies in regions in which charged particle equilibrium of the *knock-on* electrons does not exist, which is generally the case near an interface. On the other hand, its requirements viz-a-viz the B-G conditions are even more stringent than in the B-G case because S-A theory assumes that the cavity does not perturb the knock-on electron spectrum down to an energy Δ whereas B-G theory only requires this for the primary electron spectrum.

The calculation of the stopping-power ratios (spr's) needed for applying cavity theories is a complex process with a variety of difficulties.

For one thing, the parameter Δ is not well defined but is related to the energy of electrons which are fully stopped within the gas in an ion chamber. Fortunately the spr's needed for dosimetry do not depend critically on the value, and the value of $\Delta = 10$ keV has become the de facto standard.

The major difficulties concern specifying the initial source spectrum from which to calculate the relevant electron spectrum (which is usually calculated by Monte Carlo techniques but can also be done analytically for incident photon beams) and in selecting the input data for the stopping powers themselves. See Nahum, (1978), Andreo and Brahme (1986) and ICRU Report 35 concerning the state-of-the-art on calculation of spr's. The analytic calculation of the photon beam spr's used in the AAPM protocol is described in Cunningham and Schulz (1984).

4.1.9 Charge Measurement.

Let M be an ion chamber reading which is assumed to be in coulombs. M must be corrected to standard temperature and pressure conditions, i.e.

$$M = M' \left(\frac{P_o}{P} \right) \left(\frac{T + 273.2}{T_o + 273.2} \right) \quad (15)$$

where M' is the measured charge, P and P_o are the pressure and reference pressure respectively and T and T_o are the temperature and reference temperature in degrees celsius. Reference conditions are completely arbitrary and one usually uses the values defined by the standards laboratory which calibrates the ion chamber. The reference temperature, T_o , is generally 20°C in Europe and 22°C in North America (NIST, ADCL's and NRCC).

For electrometers not calibrated in terms of coulombs, the equation for M requires another correction factor f (C per meter unit), to convert the meter reading to coulombs. For a derivation which includes the electrometer's calibration factor, see RR88. In the end, the equations of clinical dosimetry are independent of the value of f because it is buried in the exposure (or air kerma) calibration factor, N_X and will be assumed to be unity here.

In dosimetry protocols, the quantity of interest is Q_{gas} , the charge liberated in the chamber. M is corrected for lack of full collection efficiency by the ion chamber

by a factor called K_{ion} defined by:

$$Q_{\text{gas}} = MK_{\text{ion}} \quad (\text{C}). \quad (16)$$

K_{ion} is greater than 1.0. For good ion chambers, it should be near unity in the calibration beam. However it can be a significant correction in other beams and the user must measure it using standard procedures discussed later.

4.1.10 Exposure and Air Kerma Calibration Factors.

Present protocols start with an exposure or air kerma calibration factor obtained from a national standards laboratory. The calibration factor relates a corrected meter reading to the exposure at the center of the chamber when the chamber is not there. It is given by:

$$N_X = \frac{X}{M^c} \quad (\text{kg}^{-1}), \quad (17)$$

where the superscript c has been introduced to specify measurements in the calibration beam at the standards lab. The equation presumes M^c has been corrected to standard temperature and pressure and holds for standard conditions of humidity, taken to be 10 to 90%^{2 3}.

The corresponding definition of the air kerma calibration factor is:

$$N_K = \frac{K_{\text{air}}}{M^c} \quad (\text{Gy/C}), \quad (18)$$

$$= N_X \left(\frac{W}{e} \right)_{\text{air}} / (1 - \bar{g}), \quad (19)$$

where the second line follows from eqn 8 relating exposure and air kerma.

4.2 Exposure and Ion Chamber Response.

4.2.1 Derivation of the Basic Equation.

The relationship between the exposure at a point and an ion chamber's response at that point will now be developed.

Assume there is CPE in the chamber's wall (i.e. there is no photon attenuation, an assumption which will be relaxed later by introducing K_{wall}). Thus:

$$D_{\text{wall}} = (K_c)_{\text{wall}} = E_\gamma \phi_\gamma \left(\frac{\overline{\mu_{\text{en}}}}{\rho} \right)_{\text{wall}} \quad (\text{Gy}). \quad (20)$$

where eqns 3 and 9 were used and ϕ_γ is the photon fluence. The assumption of charged particle equilibrium implies that the photon fluence, ϕ_γ is the same everywhere. Eventually it will be considered to be from a point source. In that case the ϕ_γ needed is that at the position of the center of the chamber when the chamber

²Some standards laboratories take reference conditions as 50% relative humidity but with an error of less than 0.15% this is equivalent to the entire range specified.

³Prior to July 1, 1990, Canadian calibration factors were defined for standard conditions of dry air and this led to some differences in the definitions. See RR88 for a complete discussion.

is not there. At distances of about 1 m from a point source, Bielajew has recently proven that the point of measurement of the chamber is very close to the center of the chamber (Bielajew, 1990b). He has also shown that this is not the case for a point source very close to the detector and has developed a method to correct for this (Bielajew, 1990a).

From the definition of $\left(\frac{W}{e}\right)_{gas}$, the energy deposited in the gas is given by $\left(\frac{W}{e}\right)_{gas} Q_{gas}$ where Q_{gas} is the charge liberated in the cavity gas. Hence:

$$D_{gas} = \left(\frac{W}{e}\right)_{gas} \frac{Q_{gas}}{m_{gas}} \quad (\text{Gy}), \quad (21)$$

where m_{gas} is the mass of the gas in the cavity.

Using eqn 7 for the exposure at the center of the ion chamber, eliminate the expression for the energy fluence in the photon beam by using eqn 20 relating the dose to the wall to the photon fluence to give:

$$X = D_{wall} \left(\frac{\overline{\mu_{en}}}{\rho}\right)_{wall}^{air} \left(\frac{e}{W}\right)_{air} \quad (\text{C/kg}). \quad (22)$$

Using the Spencer-Attix relationship, eqn 14, to eliminate D_{wall} and eqn 21 for D_{gas} to eliminate D_{gas} , gives:

$$X = \frac{Q_{gas}}{m_{gas}} \left(\frac{\overline{L}}{\rho}\right)_{gas}^{wall} \left(\frac{\overline{\mu_{en}}}{\rho}\right)_{wall}^{air} \left(\frac{W}{e}\right)_{air}^{gas} K \quad (\text{C/kg}), \quad (23)$$

where the new factor K represents a variety of corrections needed because not all the assumptions used in the derivation hold exactly.

In this fundamental equation for the exposure at a point, air refers to dry air since this appears in the definition of exposure and gas refers to the humid air or *any other gas* in the chamber.

4.2.2 Humidity Correction Factor.

It is common practice to remove references to the humid air (gas) by introducing a humidity correction factor, K_h so the previous eqn for X is:

$$X = \frac{Q_{gas}}{m_{air}} \left(\frac{\overline{L}}{\rho}\right)_{air}^{wall} \left(\frac{\overline{\mu_{en}}}{\rho}\right)_{wall}^{air} K_h K \quad (\text{C/kg}), \quad (24)$$

Note that Q_{gas} now contains the only reference to gas since the charge released is measured in humid air.

By comparison with the previous equation:

$$K_h = \frac{m_{air}}{m_{gas}} \left(\frac{W}{e}\right)_{air}^{gas} \left(\frac{\overline{L}}{\rho}\right)_{gas}^{air}. \quad (25)$$

K_h is traditionally called the humidity correction factor. However this definition holds for any gas in the chamber. As seen from fig 3, for humid air K_h is very nearly

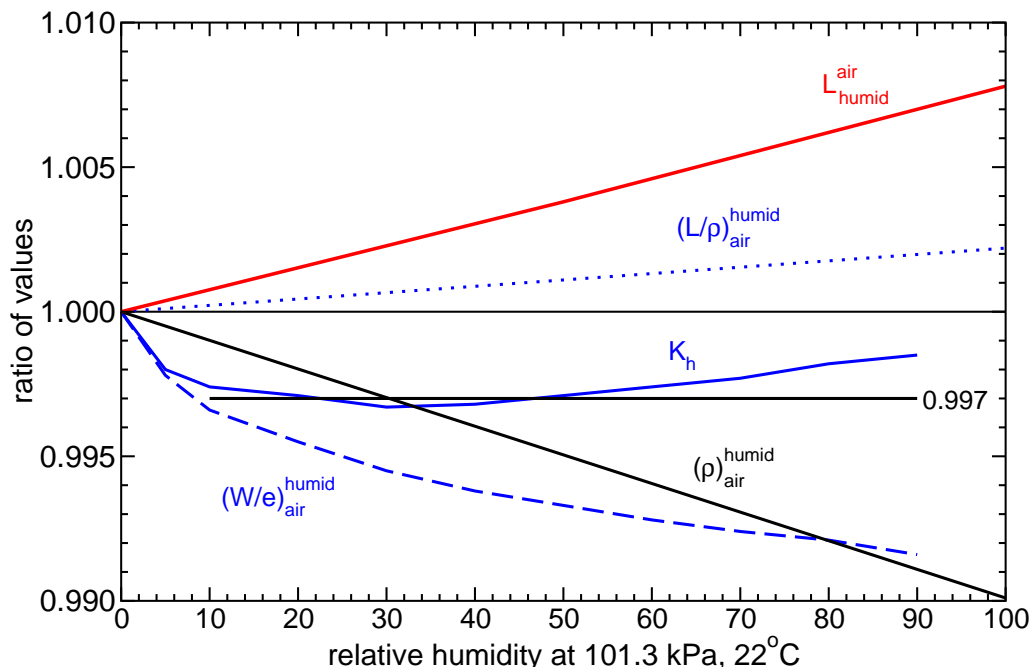


Figure 3: Variations of various physical quantities and the humidity correction factor as a function of the partial pressure of water vapour in air (from RR88).

0.997 over a wide range of humidity values thanks to cancellation of various factors⁴. Although humidity will be accounted for, hereafter the humidity will be assumed to be constant (or more importantly, K_h is constant). This assumption leads to no more than $\pm 0.15\%$ error (see section 4.5.)

The humidity correction factor considers only the direct effect of the humidity in the air. This does leave one question somewhat open, viz, what is the humidity inside an ion chamber which is in a water phantom? It is normally assumed to have the same humidity as the ambient air.

Various authors have also studied the question of water uptake by ion chambers in humid vs dry air. By changing the effective volume of the chamber, this can be a significant effect for some materials, in particular nylon (see Mijnheer, 1985, and references therein).

4.2.3 The Other Correction Factors: $K_{\text{wall}}, K_{\text{an}}, K_{\text{st}}, K_{\text{el}}, K_{\text{comp}}$.

Eqn 24 for the exposure introduced a correction factor K to account for breakdowns in various assumptions in the derivation. It has several components, viz:

$$K = K_{\text{wall}} K_{\text{an}} K_{\text{st}} K_{\text{el}} K_{\text{comp}} \quad (26)$$

K_{wall} is a correction which takes into account the lack of charged particle equilibrium in the chamber wall near the cavity, the most important aspect of which is photon attenuation and scatter in the walls of the ion chamber. It is usually greater

⁴Fortunately the stopping-power ratio is almost independent of beam quality so that this conclusion holds for all beam qualities.

than one because there is more attenuation than scatter. This factor includes the effects of electron transport and hence includes the correction β_{wall} for the center of electron production.

This factor, called $(A_{wall}\beta_{wall})^{-1}$ in the AAPM protocol, has caused many problems and has been interpreted incorrectly in a variety of ways. In particular, in the protocol the factor β_{wall} is included twice since the tabulated values of A_{wall} already include β_{wall} . This was corrected in the Letter of Clarification (Schulz *et al.*, 1986). Bielajew (1986) presented a rigorous formal proof of the fact that the Monte-Carlo calculated values of A_{wall} (called K_{wall}^{-1} here) include β_{wall} .

The actual values of A_{wall} used in the protocol were calculated by Monte-Carlo methods (Nath and Schulz, 1981). It has been shown that the Nath and Schulz calculations of ion chamber response disagree with the fundamentals of cavity theory (Nahum and Kristensen, 1982). However, it was shown that, despite the large errors in the calculations of the chamber response, the calculated A_{wall} values were correct to within $\pm 0.2\%$ (Rogers *et al.*, 1985b).

In recent work, it has been shown that the “experimentally” derived values of K_{wall} used in standards laboratories are incorrect and that the Monte-Carlo results are more accurate (Rogers and Bielajew, 1990, Bielajew, 1990c). This has significant effects on standards but little effect on values used in protocols.

As well as the above papers, Gastorf *et al.* (1986) and the IAEA Code of Practice (1987) have extensive tabulations of A_{wall} factors for many commercial chambers.

K_{an} is a correction factor to account for the $1/r^2$ decrease in the photon beam. There is some controversy over this factor, but recent work (Bielajew, 1990a,b) indicates that 1 m from a ^{60}Co source, $K_{an}=1.000$ for spherical and farmer-like cylindrical chambers and 1.001 to 1.003 for long cylindrical and pancake chambers.

K_{st} is the stem correction factor to account for the photons scattered into the chamber by the stem. It is less than or equal 1, and for chambers with small stems it can be assumed equal to unity.

K_{el} is a correction factor to account for an electrode which is made of a material different from the wall of the chamber. It is unity when the electrode is the same material as the chamber wall. For a graphite Farmer chamber with a solid 1 mm diameter electrode made of aluminium, $K_{el} \approx 0.992$. However, this correction factor is not included in current dosimetry protocols (except that of the IAEA).

The value of K_{el} for aluminium electrodes is based on the measurements of Kristensen (1983) and the Monte-Carlo calculations of Rogers *et al.* (1985b). In both cases there is a large uncertainty on the value and it is based on linear fits for chambers with larger electrodes. The value may well be larger than 0.992 (i.e. a smaller correction) since buildup effects for small diameter electrodes have not been accounted for.

If this correction is included here, a corresponding correction must be included in the dose equations. In a ^{60}Co beam the effect of the two corrections will be to cancel. The dose equation correction will partially cancel this correction in a high-energy photon beam but have no effect in an electron beam. In other words, an aluminum electrode may cause up to a 0.8% over-estimate of the dose when used in an electron

beam.

To avoid complications, it is good advice **not** to use an ion chamber with an aluminum electrode.

K_{comp} is a correction factor to account for composite wall materials in the ion chamber, i.e. to account for using a buildup cap made of material different from the wall. There are some problems with this factor (to be discussed in section 4.3.6). To avoid complications, one should use a buildup cap of the same material as the chamber wall so that $K_{\text{comp}} = 1$.

4.3 N_{gas} – The Cavity-Gas Calibration Factor.

4.3.1 Definition of N_{gas} .

Current dosimetry protocols all determine the dose to a medium by using the charge measured from an ion chamber and Spencer-Attix cavity theory which relates the dose to the gas, D_{gas} , in the ion chamber to the dose in the medium. To do this, a factor called the cavity-gas calibration factor, or just N_{gas} , is introduced to make use of the fact that:

D_{gas} can be written as the product of a corrected ion chamber output and a **constant**, the cavity-gas calibration factor, N_{gas}

more specifically:

$$D_{\text{gas}} = MK_{\text{ion}}N_{\text{gas}} \quad (\text{Gy}), \quad (27)$$

where M is the ion chamber reading in coulombs, assumed corrected to standard temperature, pressure and humidity; K_{ion} is a correction for incomplete charge collection; and N_{gas} is a constant which depends only on the ion chamber. This equation defines N_{gas} . The units are Gy/C which immediately indicates what the quantity is.

N_{gas} seems to create many problems for people. They think it is complicated. But N_{gas} is conceptually simple; it is the dose to the gas in the ion chamber per unit charge from the chamber. N_{gas} is a constant and a property of the ion chamber only (actually just the ion chamber's cavity). The real problem with N_{gas} is that the expression used to determine it is complex and the AAPM protocol does not derive the expression clearly. As a result it has several mistakes in the N_{gas} formula which leads to errors of $\approx 0.4\%$.

4.3.2 Derivation of the Expression for N_{gas} .

Rewrite eqn 27 which defines N_{gas} :

$$D_{\text{gas}}^u = M^u K_{\text{ion}}^u N_{\text{gas}} \quad (\text{Gy}), \quad (28)$$

where the superscript u is to emphasize that this equation applies in the user's beam. Eqns 21 and 16 are:

$$D_{\text{gas}} = \left(\frac{W}{e} \right)_{\text{gas}} \frac{Q_{\text{gas}}}{m_{\text{gas}}} \quad (\text{Gy}).$$

$$Q_{gas} = M^u K_{ion}^u \quad (C).$$

Solving for N_{gas} gives:

$$N_{gas} = \left(\frac{W}{e} \right)_{gas} \frac{1}{m_{gas}} \quad (\text{Gy C}^{-1}). \quad (29)$$

This equation tells us that N_{gas} is a constant which is independent of all properties of the ion chamber except the mass of gas it contains ⁵. The units suggest the definition: absorbed dose to the gas per unit charge released.

If eqn 29 could be used to get N_{gas} , there would be far fewer conceptual problems. Unfortunately it contains m_{gas} , a quantity which a clinical physicist can not normally determine directly.

To develop a more useful expression for N_{gas} , consider the user's chamber in the standards laboratory beam for calibration. Using eqn 24 for the exposure in the beam, eqn 16 for correcting the charge measurement and eqn 17 for the definition of N_X , gives:

$$N_X = \frac{Q_{gas}^c \left(\frac{\bar{L}}{\rho} \right)_{air}^{wall} \left(\frac{\mu_{en}}{\rho} \right)_{wall}^{air} K_h K}{Q_{gas}^c / K_{ion}^c}, \quad (\text{kg}^{-1}) \quad (30)$$

where the superscript c emphasizes that this equation applies to the user's chamber in the calibration beam at the standards laboratory.

Rearranging gives:

$$\frac{1}{m_{air}} = \frac{N_X}{\left(\frac{\bar{L}}{\rho} \right)_{air}^{wall} \left(\frac{\mu_{en}}{\rho} \right)_{wall}^{air} K_h K K_{ion}^c} \quad (\text{kg}^{-1}). \quad (31)$$

The definition of K_h in eqn 25 gives:

$$\frac{m_{air}}{m_{gas}} = K_h \left(\frac{W}{e} \right)_{gas}^{air} \left(\frac{\bar{L}}{\rho} \right)_{air}^{gas}, \quad (32)$$

and one can write:

$$\frac{1}{m_{gas}} = \frac{1}{m_{air}} \frac{m_{air}}{m_{gas}} \quad (\text{kg}^{-1}). \quad (33)$$

Using eqn 29 for N_{gas} and eqns 31 to 33 for $1/m_{gas}$ gives, based on the measurements in the standards laboratory:

$$N_{gas} = \frac{N_X \left(\frac{W}{e} \right)_{air}}{\left(\frac{\bar{L}}{\rho} \right)_{gas}^{wall} \left(\frac{\mu_{en}}{\rho} \right)_{wall}^{air} K K_{ion}^c} \quad (\text{Gy C}^{-1}). \quad (34)$$

In essence, the exposure calibration factor has been used to determine $1/m_{gas}$ for the user's ion chamber in order to determine N_{gas} from eqn 29. No measurements are needed at the user's site to determine N_{gas} .

⁵This is only a constant under the assumption that the humidity is a constant, an assumption which carries with it a $\pm 0.15\%$ error. See RR88 for a complete discussion and an alternative definition in terms of dry air, viz: $(W/e)_{air} \frac{1}{m_{air}}$ which really is a constant and makes no assumptions about the humidity.

By taking explicit account of humidity effects throughout the protocol and then making the assumption that the humidity correction factors remain equal, in section 4.5 it is shown that one obtains expressions for N_{gas} and D_{med} which are identical to those developed here except that the stopping-power ratios relative to air, not gas. Anticipating this result gives:

$$N_{\text{gas}} = \frac{N_X \left(\frac{W}{e}\right)_{\text{air}}}{\left(\frac{\bar{L}}{\rho}\right)_{\text{air}}^{\text{wall}} \left(\frac{\mu_{\text{en}}}{\rho}\right)_{\text{wall}}^{\text{air}} K K_{\text{ion}}^c} \quad (\text{Gy C}^{-1}). \quad (35)$$

Alternatively, this change to air can be thought of as redefining N_{gas} slightly by dividing by $\left(\frac{\bar{L}}{\rho}\right)_{\text{air}}^{\text{gas}}$ (evaluated in the calibration beam) and canceling by the same factor in the dose equation (except evaluated in the user's beam - but, at the 0.02% level, these stopping-power ratios are independent of the spectrum for which they are evaluated). In either case, one can use the stopping-power ratios evaluated relative to dry air in both equations.

4.3.3 N_{gas} in Terms of the Air Kerma Calibration Factor.

The protocol was developed at a time when NIST (the NBS) gave exposure calibration factors. Today, the calibration factors are given in terms of air kerma. Using the relationship between N_X and N_K (eqn 19) leads to the following expression for N_{gas} :

$$N_{\text{gas}} = \frac{N_K(1 - \bar{g})}{\left(\frac{\bar{L}}{\rho}\right)_{\text{air}}^{\text{wall}} \left(\frac{\mu_{\text{en}}}{\rho}\right)_{\text{wall}}^{\text{air}} K K_{\text{ion}}^c} \quad (\text{Gy C}^{-1}). \quad (36)$$

In this equation the factors are close to unity so $N_{\text{gas}} \approx N_K$. Despite this apparent simplification, the Radiation Therapy Committee of the AAPM has recommended continuing use of the equation for N_{gas} in terms of the exposure calibration factors because of the errors in the protocol concerning which value of (W/e) to use ⁶.

4.3.4 N_{gas} Compared to AAPM Values.

In the present notation, the original AAPM equation for N_{gas} is:

$$N_{\text{gas}}^{\text{AAPM83}} = \frac{N_X \left(\frac{W}{e}\right)_{50\%} \beta_{\text{wall}}}{\left(\frac{\bar{L}}{\rho}\right)_{\text{gas}}^{\text{wall}} \left(\frac{\mu_{\text{en}}}{\rho}\right)_{\text{wall}}^{\text{air}} K K_{\text{ion}}^c}. \quad (37)$$

and that from the Letter of Clarification is:

$$N_{\text{gas}}^{\text{AAPM86}} = \frac{N_X \left(\frac{W}{e}\right)_{\text{gas}}}{\left(\frac{\bar{L}}{\rho}\right)_{\text{gas}}^{\text{wall}} \left(\frac{\mu_{\text{en}}}{\rho}\right)_{\text{wall}}^{\text{air}} K K_{\text{ion}}^c K_{\text{h}}}. \quad (38)$$

The differences between the equations are significant, but cancel somewhat.

⁶Since NIST uses the correct value and the protocol uses the wrong value of (W/e) , if one uses the N_K calibration factor, one gets a different value of N_{gas} . This value is more accurate but using it would mean consistency with previous values is lost.

- Using $\left(\frac{W}{e}\right)_{50\%}$ instead of $\left(\frac{W}{e}\right)_{air}$ means N_{gas} is 0.7% low.
- The extra β_{wall} term causes a 0.5% overestimate.
- The extra K_h term increases N_{gas} by 0.3%.
- Using the stopping-power ratios for air supplied with the protocol instead of for gas would lead to a 0.1% error in N_{gas} , except, as pointed out above, there is no error in the assigned dose as long as air is used in the dose equation as well.

In summary, although it purports to use the same physical data and definitions as used here, the 1986 eqn gives a value of N_{gas} which is low for all chambers by 0.4% and hence the protocol underestimates all doses by 0.4%. Since the 1983 equation gives the same numerical results, it too underestimates N_{gas} by 0.4%.

The AAPM letter of clarification (Schulz *et al.*, 1986) noted that their equation for N_{gas} gave the same numerical values as the original 1983 equation. This is somewhat misleading because the values of physical parameters and the definition of N_X also changed in the meantime. The actual value of N_{gas} obtained using the 1983 and 1986 eqns with N_X values which were obtained in 1983 and 1986 would have changed by 1%.

4.3.5 Translation to AAPM TG-21 Notation.

For clarity, a consistent notation has been used here. The table shows the correspondence to the AAPM protocol. In the equations developed here, K represents several correction factors (see eqn 26). The protocol considers only two: K_{comp} , which it writes out explicitly, and K_{wall} .

AAPM Notation	Current Notation
$A_{wall}\beta_{wall}$	$(K_{wall})^{-1}$
A_{ion}	$(K_{ion}^c)^{-1}$
K_{humid}	K_h
written out	K_{comp}

4.3.6 Evaluation of K_{comp} .

This factor corrects for buildup cap materials different from the chamber wall material. It can be substantial. Since it is not very rigorously investigated, it is best to use a buildup cap (just for the exposure calibration) which is made of the same material as the wall, or at least as similar as possible.

Almond and Svensson (1977) suggested a formula for K_{comp} which the IAEA Code of Practice uses. For some unknown reason, the AAPM protocol uses a K_{comp} which has the inverse form from their original formula while referencing the Almond and Svensson paper. The AAPM protocol includes K_{comp} directly in the equations for N_{gas} but in the present notation, it uses:

$$K_{comp} = \frac{\alpha \left(\frac{\bar{L}}{\rho}\right)_{air}^{wall} \left(\frac{\bar{\mu}_{en}}{\rho}\right)_{wall}^{air} + (1 - \alpha) \left(\frac{\bar{L}}{\rho}\right)_{air}^{cap} \left(\frac{\bar{\mu}_{en}}{\rho}\right)_{cap}^{air}}{\left(\frac{\bar{L}}{\rho}\right)_{air}^{wall} \left(\frac{\bar{\mu}_{en}}{\rho}\right)_{wall}^{air}} \quad (39)$$

where α is the fraction of the ionization in the cavity due to electrons originating in the chamber wall and $(1-\alpha)$ is the fraction from the buildup cap.

In the limit $\alpha = 0$, i.e. the wall is replaced by the cap, K_{comp} replaces the term $\left(\frac{\bar{L}}{\rho}\right)_{\text{air}}^{\text{wall}} \left(\frac{\mu_{\text{en}}}{\rho}\right)_{\text{wall}}^{\text{air}}$ in the formula for N_{gas} with $\left(\frac{\bar{L}}{\rho}\right)_{\text{air}}^{\text{cap}} \left(\frac{\mu_{\text{en}}}{\rho}\right)_{\text{cap}}^{\text{air}}$, i.e. just what one would expect. In the limit $\alpha = 1$, i.e. no cap, K_{comp} reduces to 1 as expected.

The equation recommended by Almond and Svensson, and used in the IAEA Code of Practice is:

$$K_{\text{comp}}^{\text{AS}} = \frac{1}{\left(\frac{\bar{L}}{\rho}\right)_{\text{air}}^{\text{wall}} \left(\frac{\mu_{\text{en}}}{\rho}\right)_{\text{wall}}^{\text{air}} \left[\alpha \left(\frac{\bar{L}}{\rho}\right)_{\text{wall}}^{\text{air}} \left(\frac{\mu_{\text{en}}}{\rho}\right)_{\text{air}}^{\text{wall}} + (1 - \alpha) \left(\frac{\bar{L}}{\rho}\right)_{\text{cap}}^{\text{air}} \left(\frac{\mu_{\text{en}}}{\rho}\right)_{\text{air}}^{\text{cap}} \right]} \quad (40)$$

Although this form looks quite different, it is identical to the AAPM equation in the limit of $\alpha = 0$ and $\alpha = 1$. Furthermore, for practical cases, the numerical values of the two alternatives are virtually the same. I have no explanation for the form used in the AAPM protocol (I would like to thank Lech Papież for drawing my attention to this point). In appendix B, simplified derivations of K_{comp} and P_{wall} are given since there is considerable similarity in these factors and the confusion surrounding them.

4.3.7 α Values in a ^{60}Co beam.

The values of α in a ^{60}Co beam, which are needed in the equation for K_{comp} are presented in the protocol (fig 1). Fortunately, α is independent of the wall and buildup cap materials, as long as they are of low Z. The values of α are based on the measurements of Lempert *et al.* (1983) who measured the response of ion chambers as a function of carbon wall thickness in beams with no electron contamination. Figure 4 shows the original data. Note that the curves are extrapolated below 0.065 g cm^{-2} and the assertion that α is independent of material is based on the single point for tufnol shown as a diamond. I have done some Monte Carlo calculations of the same situation and get good agreement between the calculations and experiment for the carbon walled chamber. The extrapolation to thinner wall thicknesses is also acceptable according to the calculations and the assertion that α vs wall thickness in g/cm^2 is independent of wall material holds for the entire curve for walls of carbon, aluminum and delrin plastic.

4.3.8 Values of N_{gas} .

All the information needed to calculate N_{gas} has now been reviewed, and although it is quite complex, for a given ion chamber it needs to be done only once each time it is calibrated at a standards laboratory.

Gastorf *et al.* (1986) have calculated that the ratio $N_{\text{gas}}/(N_{\text{X}}/K_{\text{ion}}^c)$ for 27 different commercial cylindrical ion chambers with volumes varying by a factor of greater than 50. The ratio varies by less than 4%. One of the advantages of using SI is that one can see that the value of this ratio is numerically between 0 and 4% less than $(W/e)_{\text{air}}=33.97 \text{ J/C}$ instead of being some completely unphysical value.

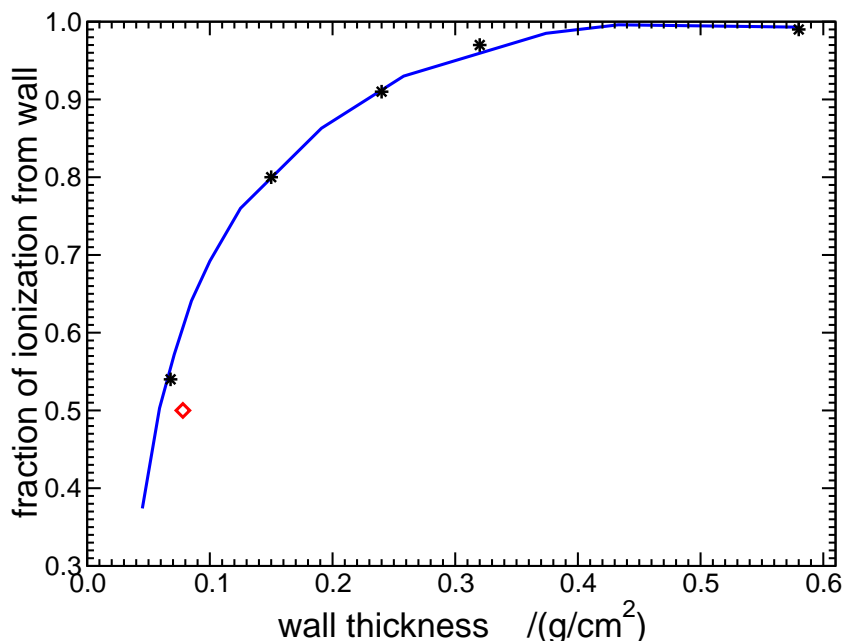


Figure 4: Experimental values of α , the fraction of ionization from the chamber's wall in a ^{60}Co beam for a graphite (stars) and delrin(diamond) -walled thimble ion chamber (from Lempert *et al.*, 1983). The solid curve is the data presented in the protocol.

4.4 The Dose to the Medium.

4.4.1 General Considerations.

For an ion chamber inserted in a medium, assuming that the chamber and cavity do not influence the electron spectrum, Spencer-Attix cavity theory gives:

$$\begin{aligned} D_{med} &= D_{gas} \left(\frac{\bar{L}}{\rho} \right)_{gas}^{med} \\ &= MP_{ion} N_{gas} \left(\frac{\bar{L}}{\rho} \right)_{air}^{med} \quad (\text{Gy}), \end{aligned} \quad (41)$$

where eqn 27 is used to expand D_{gas} , and the AAPM's notation, $P_{ion}(= K_{ion}^u)$ is used. As discussed above concerning eqn 34 for N_{gas} and in section 4.5, the *gas* in the stopping-power ratio **must** be changed to *air* under the assumption that the humidity is constant.

For any real chamber, the electron fluence spectrum is disturbed by the ion chamber. To account for these effects, the AAPM defines two correction factors, P_{wall} and P_{repl} and writes:

$$D_{med} = MN_{gas} \left(\frac{\bar{L}}{\rho} \right)_{air}^{med} P_{ion} P_{repl} P_{wall} \quad (\text{Gy}). \quad (42)$$

There are a variety of general considerations in the protocol.

- The quantity sought is dose to water, even when using plastic phantoms.
- The protocol applies to measurements in water, polystyrene or PMMA phantoms. To avoid charge buildup problems, insulating plastic phantoms should be made from slabs no greater than 1 cm thick. Non-conducting plastic phantoms allow charge to build inside them, especially when irradiated in electron beams. This stored charge can create huge electric fields which actually distort the dose distribution patterns in the phantom. For information about charge buildup in plastic phantoms see Galbraith *et al.*, (1984) and Rawlinson *et al.*, (1984).
- For electron beams, the calibration depth is restricted to d_{\max} .
- For photon beams, a series of specific recommendations concerning the calibration depths at different energies are given. They are somewhat dependent on detector characteristics. Table XI of the protocol specifies the reference depths for photon beams. They range from 5 to 10 cm or can be at d_{\max} for sufficiently small detectors.
- The point of measurement is considered to be the central axis of a cylindrical chamber or the inside of the front face of a parallel-plate chamber.
- The buildup cap should **not** be used for in-phantom measurements.

4.4.2 P_{ion} Corrections for Charge Collection.

In an ion chamber, some electrons and positive ions recombine prior to being swept from the chamber and measured as part of the charge. Techniques for determining P_{ion} , the correction factor for this effect, are based on measuring chamber response at two different voltages (see Weinhaus and Meli, 1984). P_{ion} varies with dose rate, chamber geometry and collection voltage and **must** be established for **each** calibration situation. If $P_{\text{ion}} > 1.05$, the AAPM protocol strongly recommends that the collecting voltage be increased to reduce P_{ion} or a different chamber be used with a smaller P_{ion} (in general, plane-parallel chambers have the smallest P_{ion}). It is important to keep the value of P_{ion} reasonably small, especially in pulsed, scanned beams, where P_{ion} is largest, because there is some uncertainty in the theory.

Note that P_{ion} changes along a depth-dose curve since it depends on the dose rate.

P_{ion} corrections are based on several theories of the efficiency of charge collection in ion chambers developed by Boag (see Boag, 1987 and references therein). These various theories apply to:

- continuous beams (e.g. ^{60}Co);
- pulsed beams (i.e. linear accelerator beams which are not scanned); and
- pulsed scanned beams.

The protocol recommends P_{ion} be measured for each calibration situation. The original protocol recommended using a two voltage technique to measure P_{ion} . If the chamber is used at a bias of V_1 , then the chamber response for $V_2 = \frac{1}{2}V_1$ should be measured and P_{ion} read off a graph of P_{ion} vs the measured ratios of Q_1/Q_2 . The graph is based on the theories of Boag for the three situations, and only applies for $V_2 = \frac{1}{2}V_1$.

The AAPM graph is hard to use for $P_{\text{ion}} < 1.05$, and furthermore, Boag recommended that $V_2 \leq \frac{1}{2.5} V_1$.

More recent work has made available data which apply at many voltage ratios. Use of these data was recommended in the AAPM letter of clarification (1986). In the continuous case there is a simple algebraic expression, viz:

$$P_{\text{ion}}(\text{continuous}) = \frac{\left(\frac{V_1^2}{V_2^2} - 1\right)}{\left(\frac{V_1^2}{V_2^2} - \frac{Q_1}{Q_2}\right)} \quad (43)$$

The IAEA Code of Practice's solutions for several voltage ratios are shown in fig 5.

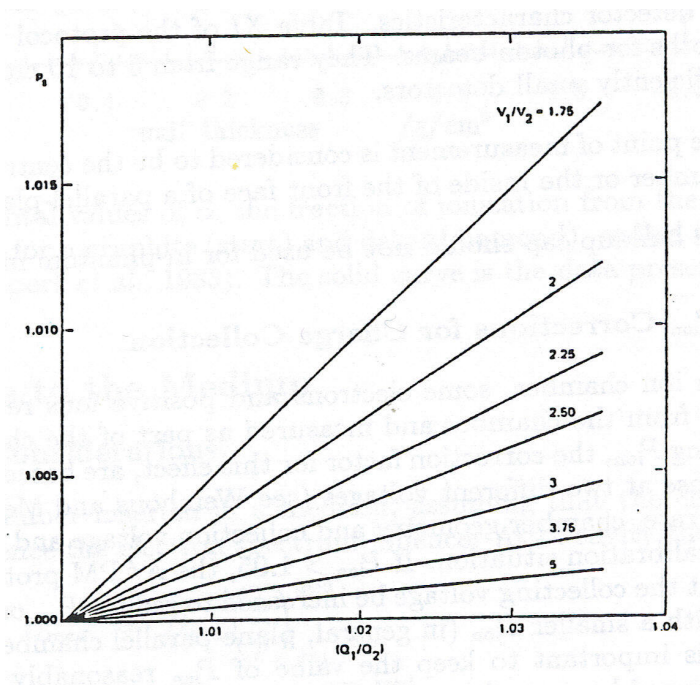


Figure 5: Solutions of eqn 43 for P_{ion} for continuous beams for a variety of voltage ratios. From the IAEA Code of Practice (1987).

In the pulsed beam cases (scanned and not) Weinhaus and Meli (1984) have provided tabulated data which give a direct method for calculating P_{ion} . They give the coefficients for the following expression:

$$P_{\text{ion}} = a_0 + a_1 \frac{Q_1}{Q_2} + a_2 \left(\frac{Q_1}{Q_2}\right)^2 \quad (44)$$

where the a_i coefficients are given for several ratios of applied biases and can be interpolated for other values.

4.4.3 P_{wall} Correction Factors.

The P_{wall} correction accounts for the walls being different from the medium and thereby changing the electron spectrum in the cavity. If the walls are the same as the medium, $P_{\text{wall}} = 1.0$.

In **electron** beams, for thin-walled chambers, $P_{\text{wall}} = 1.0$, since measurements are said to show that ion chamber response does not depend on wall composition (Johansson *et al.*, 1977). This is a basic assumption⁷ and should be valid. On the other hand, in one extreme case, Nahum *et al.* (1985) have shown it breaks down by $2.7 \pm 0.1\%$ for thin-walled graphite and aluminum chambers in a 20 MeV electron beam. Nahum (1987) has developed a theoretical model of the effect of the wall material in electron beams. It qualitatively agrees with the experimental data in the extreme case. Based on this model, Nahum has shown that the wall effect in electron beams should be less than 1%, and usually much less for situations of importance in clinical dosimetry.

For **photon** beams, Almond and Svensson's equation (1977) for P_{wall} is used:

$$P_{\text{wall}} = \frac{\alpha \left(\frac{\bar{L}}{\rho}\right)_{\text{air}}^{\text{wall}} \left(\frac{\overline{\mu_{\text{en}}}}{\rho}\right)_{\text{wall}}^{\text{med}} + (1 - \alpha) \left(\frac{\bar{L}}{\rho}\right)_{\text{air}}^{\text{med}}}{\left(\frac{\bar{L}}{\rho}\right)_{\text{air}}^{\text{med}}} \quad (45)$$

where, as in the similar equation for K_{comp} (eqn 39), α is the fraction of ionization in the cavity due to electrons from the chamber wall and $(1 - \alpha)$ is the fraction due to electrons from the dosimetry phantom.

In the limit $\alpha = 0$, i.e. no electrons from the wall, P_{wall} reduces to 1.0, as expected. In the limit $\alpha = 1.0$, the detector has become a thick-walled photon detector. Substituting $\alpha = 1.0$ in eqn 45 for P_{wall} , eqn 42 for the dose to the medium becomes:

$$D_{\text{med}} = MN_{\text{gas}} \left(\frac{\bar{L}}{\rho}\right)_{\text{air}}^{\text{wall}} \left(\frac{\overline{\mu_{\text{en}}}}{\rho}\right)_{\text{wall}}^{\text{med}} P_{\text{ion}} P_{\text{repl}}. \quad (46)$$

Here the photon detector determines D_{wall} and the $(\overline{\mu_{\text{en}}}/\rho)_{\text{wall}}^{\text{med}}$ term converts this to the dose to the medium. In other words, in this limit the expected result is also obtained.

The form recommended for P_{wall} by Almond and Svensson was not theoretically justified except as having the right limiting cases, nor was any convincing experimental data presented.

Shiragai (1978, 1979) presented a theoretical derivation of an alternative form of P_{wall} , viz:

$$P_{\text{wall}} = \frac{1}{\left(\frac{\bar{L}}{\rho}\right)_{\text{air}}^{\text{med}} \left[\alpha \left(\frac{\bar{L}}{\rho}\right)_{\text{wall}}^{\text{air}} \left(\frac{\overline{\mu_{\text{en}}}}{\rho}\right)_{\text{med}}^{\text{wall}} + (1 - \alpha) \left(\frac{\bar{L}}{\rho}\right)_{\text{med}}^{\text{air}} \right]}. \quad (47)$$

This form has been adopted by the British HPA protocol. Despite the substantially different appearance, the two formulations are identical in the limits $\alpha = 0$ or 1, and for practical values of the physical data, both forms yield essentially the same values of P_{wall} within a tenth of a percent. In Appendix B, simple derivations of both these forms are presented.

The protocol provides values for α as a function of beam energy and wall thickness in g cm^{-2} , which are again independent of wall material (protocol figure 7) as well

⁷Although the protocol references Johansson *et al.* as showing $P_{\text{wall}}=1.0$ for electron beams, this is not clear from the paper. In their paper they did assume this result, but they do not appear to present data to verify it.

as tables of $(\bar{L}/\rho)_{\text{air}}^{\text{med}}$ (Table IV) and $(\bar{\mu}_{\text{en}}/\rho)_{\text{air}}^{\text{med}}$ (Table IX) as a function of beam quality. To obtain $(\bar{\mu}_{\text{en}}/\rho)_{\text{wall}}^{\text{med}}$, one uses:

$$\left(\frac{\bar{\mu}_{\text{en}}}{\rho}\right)_{\text{wall}}^{\text{med}} = \frac{\left(\frac{\bar{\mu}_{\text{en}}}{\rho}\right)_{\text{air}}^{\text{med}}}{\left(\frac{\bar{\mu}_{\text{en}}}{\rho}\right)_{\text{air}}^{\text{wall}}} \quad (48)$$

Cunningham *et al* (1986) have investigated the variation of $(\bar{\mu}_{\text{en}}/\rho)_{\text{wall}}^{\text{water}}$ as a function of detector depth and beam size for a variety of beams. Variations of up to 1% were found. These values have been incorporated into the IAEA Code of Practice but these variations do not have a substantial effect on P_{wall} .

When a waterproofing cap is used there are three materials involved in the cavity chamber response. For this case the eqn for P_{wall} has been extended to give:

$$P_{\text{wall}} = \frac{\alpha \left(\frac{\bar{L}}{\rho}\right)_{\text{air}}^{\text{wall}} \left(\frac{\bar{\mu}_{\text{en}}}{\rho}\right)_{\text{wall}}^{\text{med}} + \tau \left(\frac{\bar{L}}{\rho}\right)_{\text{air}}^{\text{cap}} \left(\frac{\bar{\mu}_{\text{en}}}{\rho}\right)_{\text{cap}}^{\text{med}} + (1 - \alpha - \tau) \left(\frac{\bar{L}}{\rho}\right)_{\text{air}}^{\text{med}}}{\left(\frac{\bar{L}}{\rho}\right)_{\text{air}}^{\text{med}}} \quad (49)$$

where τ is the fraction of the ionization due to electrons in the cap, see e.g. Hanson and Tinoco,(1985), or Gillin *et al*, (1985).

Experimental verification of the P_{wall} corrections seems to be lacking. What data I am aware of (e.g. Andreo *et al.*, 1986, Hanson *et al*, 1985) shows discrepancies between the measurements and the theory which are comparable to the size of the predicted correction. Another problem occurs when parallel-plate chambers are used in photon beams. Here it becomes virtually impossible to define P_{wall} values because there are usually walls of different materials and thicknesses surrounding the cavity on each side. In view of the weak experimental evidence and the theoretical uncertainties in the derivation of this correction, it is clear that the P_{wall} correction factor deserves more careful investigation.

Figure 6 presents the values of P_{wall} vs beam quality for ion chambers with 0.05 g/cm² thick walls in a water phantom. The figure is based on data in the AAPM protocol.

4.4.4 A Conceptual Problem with P_{wall} and K_{comp} .

P_{wall} corrects for the lack of equivalence of the ion chamber wall and the phantom. The formulae presented above deal only with the changes due to differences in interaction coefficients. Although there is some dependence on the wall thickness through the parameter α , this in no way corrects for differences in particle attenuation and scatter in the walls. For example, in a ⁶⁰Co beam the values of P_{wall} for an ion chamber with 1 or 2 mm thick copper walls are the same ($\alpha = 1$ in both cases), despite the fact that the latter chamber would have more attenuation in a water phantom. Similarly, if using a copper-walled ion chamber in an electron beam, since a universal value of P_{fl} is used the protocol takes no account of the fact that the difference in the electron scattering in the copper walls compared to the phantom would affect the chamber response (see e.g. Nilsson *et al*, 1988).

Fortunately most ion chambers are made with thin walls and/or of tissue-like materials so that the effects mentioned here are usually negligible, but in principle they are part of the P_{wall} correction factor.

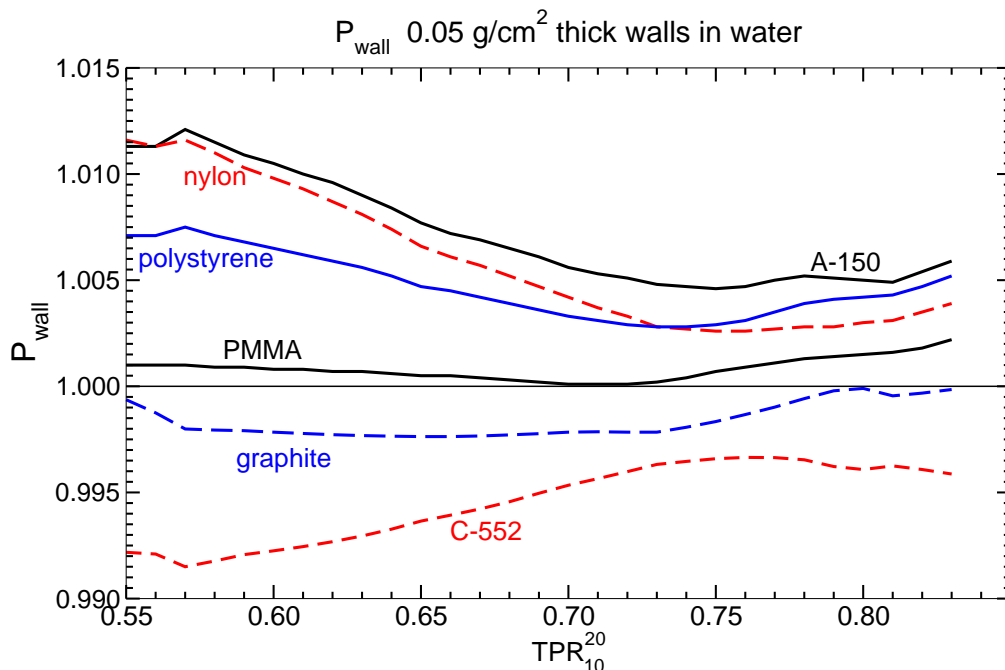


Figure 6: P_{wall} values in a water phantom vs beam quality indicated in terms of TPR_{10}^{20} for ion chambers of the different wall materials as shown and wall thickness of 0.05 g/cm^2 . Based on values in the AAPM protocol.

In the same way, in ^{60}Co in air, K_{comp} should correct the ion chamber response for differences in scatter and attenuation between the wall and buildup cap. The formula for K_{comp} does not take this into account but in this case the protocol does take this effect into account through the K_{wall} correction factor. Thus the protocol would correctly account for the differences between a 1 and 2 mm thick copper buildup cap so long as the calculated values of K_{wall} were correct.

4.4.5 Specifying Photon Beam Quality – NAP.

Factors such as $(\bar{L}/\rho)_{\text{air}}^{\text{med}}$ in the eqn for the dose to medium depend on the beam quality.

For both electron and photon beams, the AAPM protocol uses ionization measurements in the beam to be calibrated to determine a parameter which characterizes the beam quality.

Photon beam quality is characterized by the **nominal accelerating potential** (NAP) which is determined by measuring the ratio of ionization produced on the beam axis when at 10 or 20 cm depth in a water phantom at a fixed source-detector distance of 1 m, by a field which is $10 \times 10 \text{ cm}^2$ at the detector location. Figure 3 of the protocol relates the measured ionization ratio (IR) to the NAP, basically using the fact that higher energy beams are attenuated more slowly.

Attix (1984b) has pointed out that the protocol's figures 3 and 2 (which gives the relationship between stopping-power ratio, NAP and ionization ratio, IR) are inconsistent in the relationship between IR and NAP. The problem can be avoided completely by using the IR to specify beam quality directly. Andreo and Brahme

(1986) have shown that this improves consistency in dosimetry. The IAEA Code of Practice has adopted this approach.

With the AAPM protocol, the Letter of Clarification (Schulz *et al.*, Schulz *et al.*, 1986) recommended that figure 3 should be used to define NAP to allow table look ups to calculate P_{wall} . In the more critical case of determining the photon stopping-power ratio, the ionization ratio should be used with figure 2 of the letter of clarification (see fig 7).

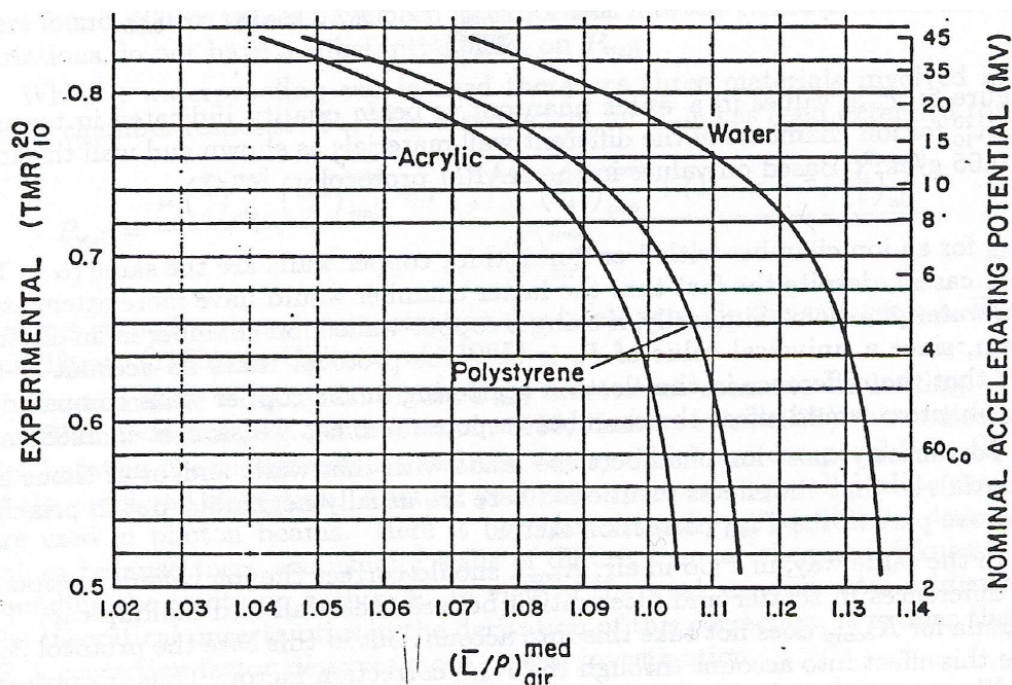


Figure 7: Figure 2 from the AAPM letter of clarification (Schulz *et al.*, 1986). It is recommended that in photon produced accelerator beams the measured value of $(\text{TMR})_{10}^{20}$ be used with this figure to determine the stopping-power ratio to use in the dose-to-medium equation.

4.4.6 Specifying Electron Beam Quality – \bar{E}_0 .

The protocol characterizes electron beams by \bar{E}_0 , the mean electron energy at the surface. For use in the dose equation, Tables V, VI and VII of the Protocol give values of $(\bar{L}/\rho)_{\text{air}}^{\text{med}}$ as a function of \bar{E}_0 , from 1 MeV to 60 MeV and as a function of depth⁸. The value of \bar{E}_0 is based on a measurement of d_{50} , the depth at which the ionization has fallen to 50% of its maximum (see fig 8) and the relationship:

$$\bar{E}_0 = 2.33d_{50} \quad (\text{MeV}) \quad (50)$$

where d_{50} is in cm and \bar{E}_0 is in MeV. There are equivalent relationships presented for use with polystyrene and PMMA phantoms.

⁸This energy range is somewhat unusual since the protocol is not recommended for use when $\bar{E}_0 < 5$ MeV. Furthermore, the data as a function of depth are misleading because, for electron beams, the protocol only applies at d_{max} , the depth of dose maximum.

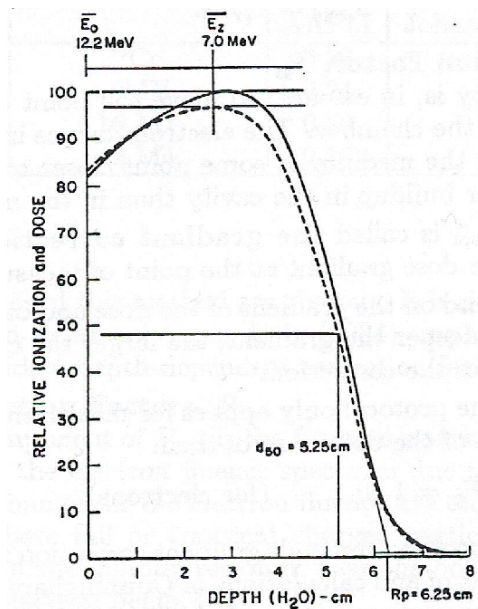


Figure 8: Revised depth-ionization (dashed) and depth-dose (solid) curves for an electron beam. The protocol determines \bar{E}_0 from d_{50} of the depth-ionization curve. R_p is used to determine the mean energy at d_{\max} for looking up fluence correction factors (see section 4.4.7). From AAPM 1986 Letter of Clarification, (Schulz *et al.*, 1986)

Wu *et al.* (1984) have pointed out that the protocol's procedure for determining \bar{E}_0 is wrong on two counts. The relationship between d_{50} and \bar{E}_0 is for d_{50} from a depth-dose curve for an incident parallel beam. Using a depth-ionization curve leads to errors of about 2% in \bar{E}_0 and not using the $1/r^2$ correction needed because the beam comes from a point source leads to errors which increase with beam energy, being over 4% at 25 MeV.

In addition, Rogers and Bielajew (1986) isolated an error in the ETRAN Monte Carlo code which had been used to determine the 2.33 MeV/cm factor in eqn 50 for \bar{E}_0 . Using more accurate calculations would further increase the assigned mean energy by roughly 400 keV at all energies.

Fortunately the final dose assigned does not depend very critically on the \bar{E}_0 and hence the problems described here have little direct effect on dosimetry except that they give incorrect beam energies.

4.4.7 The Replacement Correction Factor, $P_{\text{repl}} = P_{\text{gr}}P_{\text{fl}}$.

The insertion of a cavity into a medium causes changes in the electron spectrum. The replacement correction factor, P_{repl} , accounts for these changes. This is in contrast to P_{wall} which accounts for changes caused by the wall being different from the medium. P_{repl} can be thought of as having two components, the gradient and fluence correction factors:

$$P_{\text{repl}} = P_{\text{gr}}P_{\text{fl}}. \quad (51)$$

The Gradient Correction Factor, P_{gr} .

One effect of the cavity is, in essence, to move the point of measurement upstream

from the center of the chamber. The electron fluence in the cavity is representative of the fluence in the medium at some point closer to the source because there is less attenuation or buildup in the cavity than in the medium.

This component of P_{repl} is called **the gradient correction**, P_{gr} , because its magnitude depends on the dose gradient at the point of measurement.

These corrections depend on the gradient of the dose and on the inner diameter of the ion chamber. The steeper the gradient, the larger the correction. Also, the larger the radius, the larger the correction.

For **electrons**, since the protocol only applies for measurements at d_{max} where, by definition, the gradient of the dose is zero, then:

$$P_{\text{gr}} = 1.00. \quad (\text{for electrons})$$

For **photons**, the protocol recommends gradient correction factors based on the experimental measurements of and calculations of Cunningham and Sontag (1980). These apply only on the descending portion of photon depth-dose curves. The TG-21 committee appears to have misinterpreted the data in the reference since the data are originally shown as a function of the outer diameter of the chamber but presented in the protocol as a function of the inner diameter. Furthermore, the interpretation of the measurements is complex and the accuracy of these factors is uncertain.

In a ^{60}Co beam, for a Baldwin-Farmer chamber with an ID of 6.4 mm, values of P_{gr} in the literature vary from 0.988 (Johansson *et al.*, (1977)), to 0.989 (Cunningham and Sontag), to 0.992 (Holt *et al.*, 1979). The AAPM protocol recommends a value of 0.9918 (which reflects the mis-interpretation of Cunningham and Sontag's data). Table 2 compares the results of Johansson *et al.*, which form the basis of the equivalent correction in the IAEA Code of Practice , to those in the AAPM protocol.

Table 2:
Comparison of gradient correction factors in the AAPM protocol and Johansson *et al.*, 1977.

Beam Quality	gradient correction %/mm of cavity radius	
	AAPM	Johansson <i>et al.</i>
^{60}Co	0.27	0.40
6MV	0.24	0.40
16 MV	0.20	0.24
42 MV	0.16	0.25

Effective Point of Measurement Approach.

An alternative approach to gradient corrections is to ignore P_{gr} and to take the measurement as representing the dose at an effective point of measurement, Z_{eff} , such that the fluence spectrum in the cavity represents this point in the medium.

In the IAEA Code of Practice , for cylindrical chambers in electron and ^{60}Co beams, Z_{eff} is 0.5 r upstream of the chamber center and for high-energy photons it is 0.75 r upstream, where r is the cavity radius. These values are deduced from Johansson *et al.*'s data mentioned above.

With a plane-parallel chamber, Z_{eff} is the same as the depth of measurement, viz: the inside surface of the front wall.

The advantages of this method are obvious. It is simpler than P_{gr} and it applies away from d_{max} in electron beams. Attix (1984) emphasized this point because the simple offset avoids a depth-dependent correction factor (see fig 9).

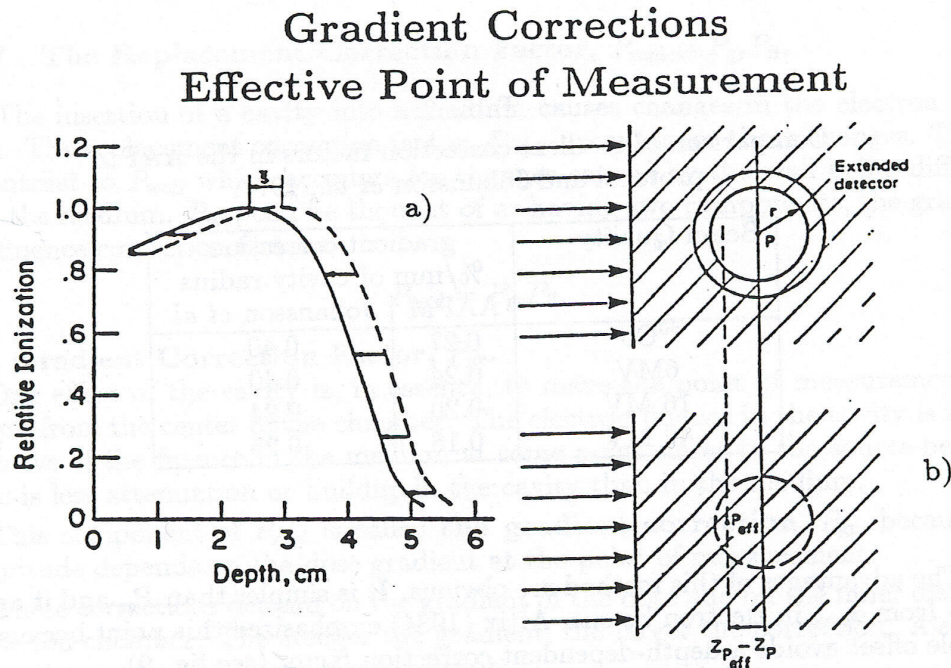


Figure 9: a) Figure showing how a simple offset in the effective point of measurement is a much simpler way to determine the dose at each depth (solid line) than to multiply the dashed curve by a gradient correction which changes significantly with depth (from Attix, 1984). b) The concept of the effective point of measurement in a phantom (from the IAEA Code of Practice).

Fluence Correction Factors, P_{fl} .

The other component of P_{repl} is the **fluence correction**, P_{fl} , which corrects for other changes in the electron fluence spectrum due to the presence of the cavity. Corrections for changes in the electron fluence are only needed if the ion chamber is in a region where full or transient charged particle equilibrium has not been established, i.e. in the buildup region or near the boundaries of a photon beam or anywhere in an electron beam.

Fluence corrections **are not required** for **photon** dose determinations made at or beyond d_{max} in a broad beam because transient electron equilibrium exists. The Fano theorem tells us that under conditions of charged particle equilibrium the electron spectrum is independent of the density in the medium (see p 255, Attix, 1986). To the extent that the cavity gas is just low-density medium material, this theorem tells us that the electron fluence spectrum is not affected by the cavity except in the sense of the gradient correction discussed above, which in essence accounts for there being transient rather than complete charged particle equilibrium. Hence no fluence

correction factor is needed in regions of transient CPE.

P_{fl} for Electron Beams

In electron beams there are two competing effects. The **in-scatter effect** which increases the fluence in the cavity because electrons are not scattered out by the gas and the **obliquity effect** which decreases the fluence in the cavity because the electrons go straight instead of scattering (see fig 10). For well designed plane-

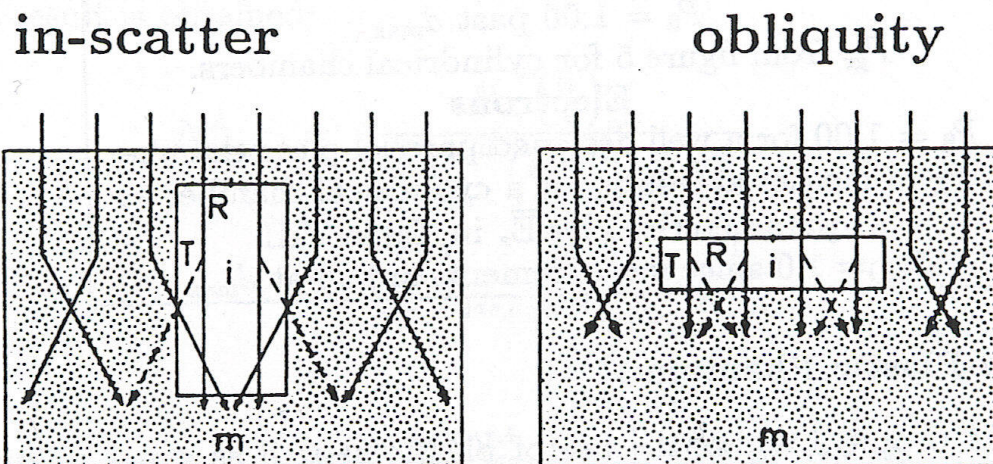


Figure 10: The electron tracks shown as dashed lines do not occur in the less dense gas in the cavity and thus in the in-scatter effect the total fluence in the cavity increases whereas for the obliquity effect the total fluence decreases (From Attix, 1986).

parallel chambers with adequate guard rings, it has been shown experimentally that $P_{fl} = 1.00$, but this is not always the case, eg. with the PTW/Markus chamber (see Mattsson *et al.*, 1981 and NCS, 1989 and references therein). Note that these results apply at d_{max} only and can not necessarily be used at other points on the depth-dose curve.

There have been calculations and measurements of P_{fl} for cylindrical chambers. Table VIII of the AAPM protocol recommends use of the values measured by Johansson *et al.* (1977). Another set of measurements have been presented recently in the Dutch electron dosimetry protocol (NCS, 1989) and Table 3 presents a comparison of these results with those of Johansson *et al.*

The values are parameterized by \bar{E}_z , the mean electron energy at the depth of measurement. In the AAPM protocol this is given by the well known Harder relationship:

$$\bar{E}_z = \bar{E}_0 \left(1 - \frac{z}{R_p}\right) \quad (52)$$

where z is the depth of measurement, R_p the practical range and \bar{E}_0 is the mean

Table 3:

Comparison of electron beam P_{fl} correction factors for Baldwin-Farmer thimble ion chambers (inner diameter of 6.3 mm) as measured by Johansson *et al.*, (1977) and as reported in the Dutch protocol (NCS, 1989).

\bar{E}_z	Johansson <i>et al.</i>	Dutch protocol
4	0.963	0.963
6	0.971	0.969
8	0.977	0.974
10	0.982	0.980
12	0.983	0.986
15	0.991	0.992
20	0.995	0.997

energy at the surface of the phantom.

$P_{fl} < 1$ which means the in-scatter dominates, making the observed fluence too large. Note that the correction is very large at low-energies or for large diameter chambers and in this case it is best to use plane-parallel chambers with large guard rings.

<p>Summary for $P_{repl} = P_{fl}P_{gr}$ Photons $P_{fl} = 1.00$ past d_{max} P_{gr} from figure 5 for cylindrical chambers.</p> <p>Electrons $P_{fl} = 1.00$ for a well designed parallel-plate chamber $P_{fl} =$ measured results for a cylindrical chamber as parameterized by \bar{E}_z in Table VIII. $P_{gr} = 1.0$ since measurements are all at d_{max}.</p>
--

4.4.8 Use of Plastic Phantoms.

The AAPM protocol allows the use of plastic as well as water phantoms although the reference dose is always the absorbed dose to water.

The depths in the phantoms must be scaled to give a water equivalent depth. In photon beams, corrections must be made for different photon scatter conditions in the plastic phantoms and in electron beams corrections must be made for changes in the electron fluence spectrum caused by the different scattering in the non-water equivalent materials. Recall the caveats earlier about charge storage in insulating plastics.

This aspect of the protocol will not be dealt with here, but there is considerable recent literature in this field. See, e.g.: Andreo *et al.*, (1984); Thwaites, (1985); Mattsson and Nahum (1984); Bruinvis *et al.*, (1985), Ten Haken and Fraass, (1987); and Grosswendt and Roos (1989).

4.5 Exact Treatment of Humidity Effects.

Up to this point, humidity effects have been accounted for but the humidity has been assumed to stay constant. If humidity effects are accounted for throughout the derivation, the following results are obtained (RR88):

$$N_{gas,u}^{exact} = \frac{N_X \left(\frac{W}{e}\right)_{air} \left(\frac{\bar{L}^u}{\rho}\right)_{air}^{gas,u} K_h^u}{\left(\frac{\bar{L}^c}{\rho}\right)_{air}^{wall} \left(\frac{\bar{\mu}_{en}}{\rho}\right)_{wall}^{air} K K_{ion}^c K_h^c} \quad (53)$$

$$= \left(\frac{W}{e}\right)_{gas,u} \frac{1}{m_{gas}^u} \quad (\text{Gy C}^{-1}) \quad (54)$$

$$D_{med} = M^u N_{gas,u}^{exact} \left(\frac{\bar{L}^u}{\rho}\right)_{gas,u}^{med} K_{ion}^u P_{repl} P_{wall} \quad (55)$$

One feature of eqn 53 is that it maintains the original definition of N_{gas} , viz the absorbed dose to the gas in the cavity per unit charge liberated. Unfortunately, this means N_{gas} is no longer a constant, it depends slightly on the humidity at the time of use.

Note that the stopping-power ratios have their dependence on the beam quality (c or u) made explicit and the ratio of humidity factors is unity to $\pm 0.15\%$.

By assuming that the humidity correction factors are equal to each other at this point instead of at the beginning of the derivation, after slight rearranging a useful result is obtained:

$$N_{gas,u}^A = \frac{N_X \left(\frac{W}{e}\right)_{air}}{\left(\frac{\bar{L}^c}{\rho}\right)_{air}^{wall} \left(\frac{\bar{\mu}_{en}}{\rho}\right)_{wall}^{air} K K_{ion}^c} \quad (56)$$

$$= \left(\frac{W}{e}\right)_{gas,c} \left(\frac{\bar{L}^c}{\rho}\right)_{gas,c}^{air} \frac{1}{m_{gas}^c} \quad (\text{Gy C}^{-1}) \quad (57)$$

$$D_{med} = M^u N_{gas}^A \left(\frac{\bar{L}^u}{\rho}\right)_{air}^{med} K_{ion}^u P_{repl} P_{wall} \quad (58)$$

In eqn 57, the definition of N_{gas} is no longer simple, but eqn 56 for determining it is much simpler. In fact it is identical to the eqn 34 derived above except with the gas term changed to air . This is the result anticipated in eqns 35 and 41. Furthermore, it is a constant for a given calibration.

The error introduced by assuming K_h remains constant is $\pm 0.15\%$ (see RR88).

4.6 Stopping Power Inconsistencies.

There is considerable inconsistency in the AAPM protocol concerning use of physical data, especially electron stopping powers and stopping-power ratios (spr's).

For **electron** beams, the spr's are based on ICRU Report 37 values. These are also used by the IAEA, but differ by up to 1.3% from the values used in ICRU

Report 35 on electron dosimetry (which used stopping powers based on Sternheimer and Peierls (1971) S&P71).

For **photon** beams, the AAPM protocol uses spr 's based on the S&P71 stopping powers. This can lead to inconsistencies of up to 1%. For example, $(\bar{L}/\rho)_{\text{air}}^{\text{carbon}}$ differs by 1% from the ICRU-37 value which is used in the NIST exposure standard and this leads to a 1% error in N_{gas} for an ion chamber made completely of carbon. For a more complete discussion, see Rogers *et al.*, (1985a), Andreo (1988) and Mijnheer and Chin (1989).

The overall situation is very complex, but rarely leads to errors as large as 1%. In contrast, the IAEA Code of Practice uses a consistent set of data based on the work of Andreo *et al.* (1986).

5 The IAEA Code of Practice .

The IAEA Code of Practice, “*Absorbed Dose Determination in Photon and Electron Beams: An International Code of Practice.*”, was published in 1987 as Report 277 of the IAEA’s Technical Report Series. The principle authors were Pedro Andreo, Jack Cunningham (a member of TG-21), Klaus Hohlfield and Hans Svensson with guidance and advice from a variety of quarters, including Suntha Suntheralingham of the AAPM TG-21 committee.

It is available from the Division of Publications of the IAEA, Wagramerstrasse 5, P.O. Box 100, A-1400 Vienna, Austria for 240 Austrian shillings.

It is a 98 page book with a scope roughly equivalent to the AAPM protocol with an added feature being that it covers x-ray beams in the energy range 10 kV to 300 kV. This latter component gives a procedure which lead to dose assignments in low-energy beams which are up to 10% different from those given by the procedure in the old ICRU 23 protocol. This aspect of the protocol is at best controversial and has some minor errors in it, and at worst, is just plain wrong. Until the dust settles, one should stick to the ICRU 23 protocol for the low energy region, despite the known problems with it.

5.1 Fundamentals of the IAEA Code of Practice.

The physics and approach of the IAEA Code of Practice is very similar to that of the AAPM protocol and in fact gives the same assigned dose to within 1% in the vast majority of comparisons reported so far. The IAEA Code of Practice has removed many of the errors in the AAPM protocol and has the advantage of using a consistent set of physical data throughout the protocol. Thus despite the similarity in the final dose numbers assigned, the IAEA Code of Practice is preferable because it is more logical and therefore more easily understood, thus reducing the chances of error. Its procedure also applies at depths other than d_{max} in an electron beam, an unfortunate restriction of the AAPM protocol.

The protocol includes a useful table with the physical characteristics of many commercial ion chambers (see their Table II).

5.2 Phantom Material.

For photon beams, the protocol only applies to water phantoms, unlike the AAPM protocol which allows for measurements in other phantoms. The IAEA and AAPM protocols both allow for the use of plastic phantoms in electron beams although they use different approaches to deduce the absorbed dose to water. In both protocols the reference dose is to water.

5.3 Beam Quality and Average Energy Specification.

5.3.1 Electrons.

For the purpose of finding stopping-power ratios, the IAEA Code of Practice specifies electron beam quality by the mean energy at the surface given by:

$$\bar{E}_o = 2.33R_{50} \quad [\text{MeV}] \quad (59)$$

where R_{50} is the depth in cm at which the absorbed dose falls to 50% of dose maximum in a broad parallel (i.e. infinite SSD) beam.

This is similar to, but distinct from the AAPM procedure which applies to depth-ionization curves uncorrected to an infinite SSD instead of to depth-absorbed dose curves. The IAEA procedure is more accurate in estimating the mean beam energy but the differences in the assigned dose are negligible (see section 4.4.6).

To determine the mean energy, \bar{E}_z , at a depth z in a phantom irradiated by an electron beam, rather than using the well known Harder relationship used by the AAPM, viz:

$$\bar{E}_z = \bar{E}_o(1 - z/R_p) \quad (60)$$

where z is the depth in cm and R_p is the practical range in cm, the IAEA Code of Practice uses the results of Monte Carlo calculations and presents a table of values. This can lead to 10 or 15% changes in the assigned energy but this doesn't play any role in the final dose assignment because it only enters in determining the perturbation factor, p_u ($=P_R$ in the AAPM protocol) and the IAEA had to adjust the tables to reflect the fact that the original data were determined using Harder's relationship.

5.3.2 Photons.

The IAEA specifies its photon beam quality in terms of the ratio of dose measurements at depths in phantom of 10 and 20 cm at a constant source-to-detector distance of about 100 cm and for a 10x10 cm² field in the plane of the detector. This measures the ratio of doses in a parallel beam and is referred to as TPR_{10}^{20} (short for Tissue Phantom Ratio). The IAEA uses this parameter to select stopping-power ratios for photon beams.

In contrast, the AAPM introduces the Nominal Accelerating Potential (NAP) which is found from the TPR_{10}^{20} and then uses the NAP to find the appropriate stopping-power ratio. This procedure could in principle be equivalent, but in practice isn't because the IAEA data is based on a more recent and more detailed analysis.

5.4 IAEA Formalism.

The IAEA starts from an air kerma calibration factor, N_K , rather than the exposure calibration factor N_X used in the AAPM protocol (this should make no difference, but in the AAPM protocol the confusion over correct W/e values has muddied the water).

The IAEA defines N_D in the same way as the AAPM define N_{gas} and relates it to the air kerma calibration factor via:

$$N_D = N_K(1 - g)k_{\text{att}}k_m \quad [\text{Gy/C}] \quad (61)$$

where $k_{\text{att}} = K_{\text{wall}}^{-1} = A_{\text{wall}}\beta_{\text{wall}}$ in the notation of section 4 or the AAPM protocol respectively, and with:

$$k_m = \alpha s_{\text{air,wall}} (\overline{\mu_{\text{en}}}/\rho)_{\text{air}}^{\text{wall}} + (1 - \alpha) s_{\text{air,cap}} (\overline{\mu_{\text{en}}}/\rho)_{\text{air}}^{\text{cap}} \quad (62)$$

where α is the fraction of the ionization inside the air cavity due to electrons from the chamber wall and $s_{\text{air,wall}} = (\overline{L}/\rho)_{\text{wall}}^{\text{air}}$ is the same Spencer-Attix stopping-power ratio as in the AAPM protocol, just in different notation.

The IAEA uses the same values of k_{att} and α as the AAPM protocol. The parameter k_m should be equivalent to the following:

$$k_m = (\overline{L}/\rho)_{\text{wall}}^{\text{air}} (\overline{\mu_{\text{en}}}/\rho)_{\text{air}}^{\text{wall}} / K_{\text{comp}} \quad (63)$$

because the article referenced for the basic equation is the same. However this equation doesn't hold because the AAPM interpreted the reference for K_{comp} incorrectly (as discussed in section 4.3.6). Nonetheless, for all practical chambers there is only a negligible difference in the numerical values implied by the equations.

The IAEA provides the basic data to calculate the factor k_m but also provides a table for many commercial chambers with values of k_{att} , k_m and their product (see table XVIII).

Note that this approach to determining N_{gas} , i.e. N_D here, is much simpler than in the AAPM protocol because it starts from N_K and hence $(\frac{W}{e})$ doesn't enter. In fact, N_D is equal to N_K within a few percent for most chambers.

Note also that the IAEA assumes that the ion collection efficiency in the calibration laboratory, K_{ion}^c is unity. This is an accurate assumption which also must be made when using the AAPM protocol.

5.5 IAEA Equation for the Dose to the Medium.

The basic dose to medium equation is different from that of the AAPM in several ways.

$$D_w(P_{\text{eff}}) = M_u N_D s_{w,\text{air}} p_u. \quad (64)$$

The first major difference is that the dose in the water is determined at an effective point of measurement, not the center of the cavity as in the AAPM protocol (for cylindrical chambers at least). See the discussion in section 4.4.7.

The factor p_u corrects for several effects, corrected for by P_{fl} and P_{wall} in the AAPM protocol.

The factor p_u for photons is given by the same equations as P_{wall} in the AAPM protocol, but uses a more consistent set of stopping-power data, specifies beam quality in terms of TPR_{10}^{20} and uses $(\overline{\mu_{en}}/\rho)$ values which take into account the effects of the phantom on the spectrum (using the work of Cunningham et al, 1986). For photon beams, P_{fl} is taken as 1.00 in both protocols.

In electron beams, P_{wall} is taken as unity in both protocols and in this case p_u is the same as P_{fl} in the AAPM, based on the work of Johansson et al (1977) which gives a table for cylindrical chambers and asserts that it is unity for parallel plate chambers.

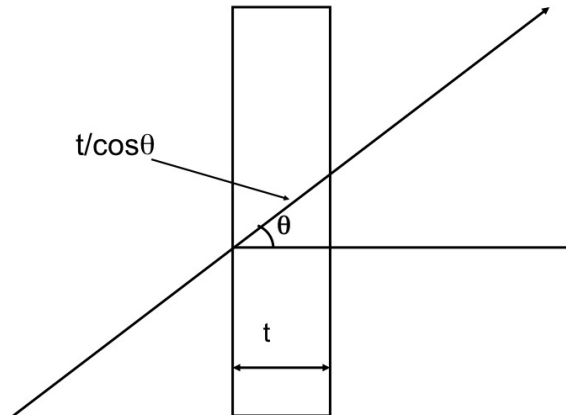
One last item that the IAEA considers, but which the AAPM ignores completely, is that for chambers with aluminium electrodes, there should be a correction taken into account (see section 4.2.3). The IAEA Code of Practice introduces a correction factor which amounts to a 0.8% increase in electron beams, an 0.4% increase for photon beams above 25 MV but no change in lower energy photon beams. Strictly speaking they have introduced this correction factor incorrectly since it should affect the value of N_D in all cases in which there is an aluminium electrode and then be exactly cancelled in low energy photon beams by another correction in the dose equation. However, the method adopted is simpler in the vast majority of cases.

6 Acknowledgements.

These notes and my understanding of dosimetry protocols have been strongly influenced by the ideas of, and my conversations with my colleagues at NRC, in particular Carl Ross, Alex Bielajew and Ken Shortt, and my colleagues Alan Nahum of the Royal Marsden Hospital and Pedro Andreo of the Karolinska Institute. I thank them all.

7 Appendices.

7.1 A: Proof of Fluence and Dose Equation.



Consider an electron passing through a slab of area dA cm^2 and thickness t cm. For the moment, assume secondary electrons lose their energy on the spot. The path-length in the volume is $\frac{t}{\cos(\theta)}$. The electron mass collision stopping power, $(S/\rho)_{col}$, gives the energy lost to electrons in the material per unit pathlength (in g cm^{-2}). The energy deposited in the slab is given by:

$$E_{dep} = \frac{\rho t}{\cos(\theta)} (S/\rho)_{col}. \quad (65)$$

In this simple case, the particle fluence (using the “pathlength per unit volume” definition, see section 4.1.1) is given by:

$$\Phi = \frac{\frac{t}{\cos(\theta)}}{tdA} = \frac{1}{dA \cos(\theta)}. \quad (66)$$

Substituting this into eqn 65 gives:

$$E_{dep} = \Phi dA \rho t (S/\rho)_{col}. \quad (67)$$

From this we find:

$$D = \frac{E_{dep}}{mass} = \frac{\Phi dA \rho t (S/\rho)_{col}}{\rho t dA} = \Phi (S/\rho)_{col}.$$

This important relationship between fluence and dose holds for arbitrary volumes and fluences in any direction.

The derivation assumes that radiative photons escape from the volume of interest and secondary electrons are absorbed on the spot. This latter condition doesn't hold, but in conditions of **charged particle equilibrium of secondary electrons**, the result is still valid because energy transported out of the volume by knock-on electrons is replaced by similar ones coming in.

7.2 B: Derivations of K_{comp} and P_{wall} .

P_{wall} is a factor in the dose to medium equation for photon beams which corrects for the effects of the chamber wall being different from the medium.

For an ideal case in which the chamber had no wall:

$$D_{\text{water}} = D_{\text{gas}} \left(\frac{\bar{L}}{\rho} \right)_{\text{gas}}^{\text{water}} \quad (68)$$

For the case in which it had a thick wall:

$$D_{\text{water}} = D_{\text{gas}} \left(\frac{\bar{L}}{\rho} \right)_{\text{gas}}^{\text{wall}} \left(\frac{\mu_{\text{en}}}{\rho} \right)_{\text{wall}}^{\text{water}} \quad (69)$$

where one uses of the Spencer-Attix eqn (14) to obtain the dose to the wall from the dose to the gas and uses eqn 10 to relate the dose to the wall to the dose to the water in the same photon fluence (which holds if there is transient charged particle equilibrium).

Almond and Svensson (1977) assert that the actual dose to water is a summation of these two components to give:

$$D_{\text{water}} = D_{\text{gas}} \left(\alpha \left(\frac{\bar{L}}{\rho} \right)_{\text{gas}}^{\text{wall}} \left(\frac{\mu_{\text{en}}}{\rho} \right)_{\text{wall}}^{\text{water}} + (1 - \alpha) \left(\frac{\bar{L}}{\rho} \right)_{\text{gas}}^{\text{water}} \right) \quad (70)$$

where α is the fraction of ionization in the gas coming from electrons starting in the wall and $(1-\alpha)$ is the fraction coming from the water. From the definition of P_{wall} , this immediately leads to the equation used in the TG-21 protocol, viz:

$$P_{\text{wall}} = \frac{\alpha \left(\frac{\bar{L}}{\rho} \right)_{\text{air}}^{\text{wall}} \left(\frac{\mu_{\text{en}}}{\rho} \right)_{\text{wall}}^{\text{med}} + (1 - \alpha) \left(\frac{\bar{L}}{\rho} \right)_{\text{air}}^{\text{med}}}{\left(\frac{\bar{L}}{\rho} \right)_{\text{air}}^{\text{med}}} \quad (71)$$

This derivation isn't really logical since the dose to the water does not have two components. However, the dose to the gas does! From this perspective, the following derivation is obtained (I was shown this by my colleague Carl Ross but it is derived by Shiragai(1978,1979) and others).

First write the dose to the gas in the chamber in term of its two physically distinct components:

$$D_{\text{gas}} = D_{\text{gas}}(\text{wall}) + D_{\text{gas}}(\text{water}). \quad (72)$$

where wall and water indicate the components arising from electrons set in motion by photon interactions in the wall or the water. If all the electrons were from the wall:

$$D_{\text{gas}}^o(\text{wall}) = D_{\text{water}} \left(\frac{\bar{L}}{\rho} \right)_{\text{wall}}^{\text{gas}} \left(\frac{\mu_{\text{en}}}{\rho} \right)_{\text{water}}^{\text{wall}} \quad (73)$$

where the ratio of mass-energy absorption coefficients converts the dose to the water to the dose in the wall (under the assumption of transient charged particle equilibrium

and using eqn 10) and the stopping-power ratio converts this to the dose to the gas (using eqn 14). If all the electrons were from the water, one would have:

$$D_{\text{gas}}^o(\text{water}) = D_{\text{water}} \left(\frac{\bar{L}}{\rho} \right)_{\text{water}}^{\text{gas}} \quad (74)$$

where it is assumed that the wall does not affect the electron spectrum from the water.

In reality, the component from the wall and water are only some fraction of these components, i.e.:

$$D_{\text{gas}}(\text{wall}) = \alpha D_{\text{gas}}^o(\text{wall}) \quad (75)$$

and

$$D_{\text{gas}}(\text{water}) = \beta D_{\text{gas}}^o(\text{water}) \quad (76)$$

Combining these equations gives:

$$D_{\text{gas}} = D_{\text{water}} \left(\alpha \left(\frac{\bar{L}}{\rho} \right)_{\text{wall}}^{\text{gas}} \left(\frac{\mu_{\text{en}}}{\rho} \right)_{\text{water}}^{\text{wall}} + \beta \left(\frac{\bar{L}}{\rho} \right)_{\text{water}}^{\text{gas}} \right) \quad (77)$$

If we consider the case in which the wall is made of water, then:

$$D_{\text{gas}} = D_{\text{water}} \left(\frac{\bar{L}}{\rho} \right)_{\text{water}}^{\text{gas}} (\alpha + \beta). \quad (78)$$

Hence, we must have $\alpha + \beta = 1$. The approximation is then made that this will hold for any wall material and hence:

$$D_{\text{gas}} = D_{\text{water}} \left(\alpha \left(\frac{\bar{L}}{\rho} \right)_{\text{wall}}^{\text{gas}} \left(\frac{\mu_{\text{en}}}{\rho} \right)_{\text{water}}^{\text{wall}} + (1 - \alpha) \left(\frac{\bar{L}}{\rho} \right)_{\text{water}}^{\text{gas}} \right). \quad (79)$$

which leads to:

$$P_{\text{wall}} = \frac{1}{\left(\frac{\bar{L}}{\rho} \right)_{\text{air}}^{\text{water}} \left(\alpha \left(\frac{\bar{L}}{\rho} \right)_{\text{wall}}^{\text{air}} \left(\frac{\mu_{\text{en}}}{\rho} \right)_{\text{water}}^{\text{wall}} + (1 - \alpha) \left(\frac{\bar{L}}{\rho} \right)_{\text{water}}^{\text{air}} \right)}. \quad (80)$$

This is the form developed by Shiragai (1978, 1979). It has been adopted in the British HPA protocol. Despite the substantially different appearance, the two formulations are identical in the limits $\alpha = 0$ or 1 , and for practical values of the physical data, both forms yield essentially the same values of P_{wall} .

The distinction between the two formulations of P_{wall} is reasonably straightforward and the use of each formulation is made clear in each protocol. This is not the case for the factor K_{comp} . One can derive the following form for K_{comp} using exactly analogous arguments which start from considering the dose to the gas in an ion chamber exposed free in air to be made up of components from the cap and the wall:

$$K_{\text{comp}} = \frac{1}{\left(\frac{\bar{L}}{\rho} \right)_{\text{air}}^{\text{wall}} \left(\frac{\mu_{\text{en}}}{\rho} \right)_{\text{wall}}^{\text{air}} \left[\alpha \left(\frac{\bar{L}}{\rho} \right)_{\text{wall}}^{\text{air}} \left(\frac{\mu_{\text{en}}}{\rho} \right)_{\text{air}}^{\text{wall}} + (1 - \alpha) \left(\frac{\bar{L}}{\rho} \right)_{\text{cap}}^{\text{air}} \left(\frac{\mu_{\text{en}}}{\rho} \right)_{\text{air}}^{\text{cap}} \right]} \quad (81)$$

This is exactly the equation recommended by Almond and Svensson (1977) and given above as eqn 40. In other words, the two equations recommended by Almond and Svensson for K_{comp} and P_{wall} are not consistent. Their equation for K_{comp} is consistent with Shiragai's equation for P_{wall} .

This issue is even more complicated because the AAPM referenced the Almond and Svensson paper for their equation for K_{comp} but used a formulation which looks more like the Almond and Svensson formulation of P_{wall} . In some senses, this is all a tempest in a tea-pot since both formulations give the same numerical results. Nonetheless, there is needless confusion.

7.3 Appendix C

Table of contents took 2 pages here in the original.

8 References.

AAPM TG-21,(1983) *A protocol for the determination of absorbed dose from high energy photon and electron beams*, Med. Phys. **10** 741, also there is an erratum for figure 6, Med. Phys. **11** (1984) 213.

P.R. Almond and H. Svensson, *Ionization chamber dosimetry for photon and electron beams. Theoretical considerations*, Acta Radiologica, Therapy, Physics and Biology **16** (1977) 177.

P. Andreo, (1988). *Consistency in Stopping-Power Ratios for Dosimetry*, in “Dosimetry in Radiotherapy”, (IAEA, Vienna) Vol 1, 3 – 11.

P. Andreo and A. Brahme, (1986). *Stopping-power data for high-energy photon beams*, Phys. Med. Biol. **31** 839.

P. Andreo, A.E. Nahum and A. Brahme, (1986). *Chamber-dependent wall correction factors in dosimetry*, Phys. Med. Biol. **31** 1189.

P. Andreo, A. Hernandez, Esther Millan and Santiago Millan, (1984). *Comments on the transfer of absorbed dose from plastic to water in electron beams*, Med. Phys. **11** 874 – 876.

F.H. Attix, (1979). *The partition of kerma to account for bremsstrahlung*, Health Phys. **36** 347.

F.H. Attix, (1984). *A simple derivation of N_{gas} , a correction in A_{wall} , and other comments on the AAPM Task Group 21 protocol*, Med. Phys. **11** 725.

F.H. Attix, (1984b). *Presentation on nominal accelerating potential as a function of the ionization ratio in the AAPM dosimetry protocol*. Med. Phys. **11** 565 – 566.

F.H. Attix, (1986) *Introduction to Radiological Physics and Radiation Dosimetry*, (Wiley, New York).

A.F. Bielajew, (1986). *Ionization cavity theory: A formal derivation of perturbation factors for thick walled ion chambers in photon beams*, Phys. Med. Biol. **31** 161.

A.F. Bielajew, (1990a). *Correction factors for thick-walled ionisation chambers in point-source photon beams*, Phys. Med. Biol. **35** 501 – 516.

A.F. Bielajew, (1990b). *An analytic theory of the point-source non-uniformity correction factor for thick-walled ionisation chambers in photon beams*, Phys. Med. Biol. **35** 517 – 538.

A.F. Bielajew, (1990c). *On the technique of extrapolation to obtain wall correction factors for ion chambers irradiated by photon beams*. submitted to Med. Phys., Oct 1989.

M. Boutillon and A.M. Perroche-Roux, (1987). *Re-evaluation of the W value for electrons in dry air*. Phys. Med. Biol. **32** 213 – 219.

- I.A.D. Bruinvis, S. Heukelom and B.J. Mijnheer, (1985). *Comparison of ionization measurements in water and polystyrene for electron beam dosimetry*, Phys. Med. Biol. **30** 1043 – 1053.
- J.W. Boag, (1987). *Ionization Chambers* in “The Dosimetry of Ionizing Radiation”, Eds K.R. Kase, B.E. Bjarngard and F.H. Attix, (Academic Press), Vol II, 169–244.
- A.B. Chilton, (1978). *A Note on the Fluence Concept*, Health Phys. **34** 715-716.
- A.B. Chilton, (1979). *Further Comments on an Alternative Definition of Fluence*, Health Phys. **35** 637–638.
- J.R. Cunningham, M. Woo, D.W.O. Rogers and A.F. Bielajew, (1986). *The dependence of mass energy absorption coefficient ratios on beam size and depth in a phantom*, Med. Phys. **13** 496 – 502.
- J.R. Cunningham and R.J. Schulz, (1984). *On the selection of stopping-power and mass-energy absorption coefficient ratios for high energy x-ray dosimetry*, Med. Phys. **11** 618 – 623.
- J.R. Cunningham and M.R. Sontag, (1980). *Displacement Corrections Used in Absorbed Dose Determinations*. Med. Phys. **7** 672 – 676.
- D.M. Galbraith, J. A. Rawlinson and P. Munro, (1984). *Dose errors due to charge storage in electron irradiated plastic phantoms*, Med. Phys. **11** 197 – 203.
- R. Gastorf, L. Humphries, M. Rozenfeld (1986). *Cylindrical chambers dimensions and the corresponding values of A_{wall} and $N_{\text{gas}}/(N_{\text{X}}/A_{\text{ion}})$* , Med. Phys. **13** 751 – 754.
- M.T. Gillin, R.W. Kline, A Niroomand-Rad and Daniel F. Grimm, (1985). *The effect of thickness of the waterproofing sheath on the calibration of photon and electron beams*, Med. Phys. **12** 234 – 236.
- B. Grosswendt and M. Roos, (1989). *Electron beam absorption in solid and water phantoms: depth scaling and energy-range relations*, Phys. Med. Biol. **34** 509 – 518.
- W.F. Hanson, J.A.D Tinoco (1985). *Effects of plastic protective caps on the calibration of therapy beams in water*, Med. Phys. **12** 243 – 248.
- J.G. Holt, R.C. Fleischman, D.J. Perry and A. Buffa, (1979). *Examination of the factors A_c and A_{eq} for cylindrical ion chambers used in ^{60}Co beams*, Med. Phys. **6** 280 – 284.
- ICRU Report 14, (1969) *Radiation Dosimetry: X Rays and Gamma Rays with Maximum Photon Energies Between 0.6 and 50 MeV*. (ICRU, Washington D.C.)
- ICRU Report 31, (1979). *Average Energy Required to Produce an Ion Pair*, (ICRU, Washington D.C.)
- ICRU Report 35, (1985) *Radiation Dosimetry: Electron beams with energies between 1 and 50 MeV*, (ICRU, Washington D.C.)
- ICRU Report 37, (1984) *Stopping Powers for Electrons and Positrons*, (ICRU, Washington D.C.)

- K.A. Johansson, L.O. Mattsson, L. Lindborg and H. Svensson, (1977). *Absorbed-dose determination with ionization chambers in electron and photon beams having energies between 1 and 50 MeV*, IAEA Symposium Proceedings, (Vienna) IAEA-SM-222/35, 243–270.
- M. Kristensen, (1983). *Measured influence of the central electrode diameter and material on the response of a graphite ionization chamber to ^{60}Co gamma-rays*, Phys. Med. Biol. **28** 1269.
- G.D. Lempert, R. Nath and R.J. Schulz, *Fraction of ionization from electrons arising in the wall of an ion chamber*. Med. Phys. **10** 1 – 3.
- L.O. Mattsson, K.A. Johansson and H. Svensson, *Calibration and use of plane-parallel ionization chambers for the determination of absorbed dose in electron beams*. Acta Rad. Oncol. **20** 385 – 399.
- L.O. Mattsson and A.E. Nahum, (1984). *Concerning comparisons of electron beam absorbed dose measurements in water and polystyrene*, Med. Phys. **11** 85 – 87.
- B.J. Mijnheer and L.M. Chin, (1989). *The effect of differences in data base on the determination of absorbed dose in high-energy photon beams using the AAPM protocol*, Med. Phys. **16** 119.
- B.J. Mijnheer, (1985). *Variations in response to radiation of a nylon-walled ionization chamber induced by humidity changes*, Med. Phys. **12** 625.
- NACP, 1980. *Procedures in external beam radiotherapy dosimetry with photon and electron beams with maximum energies between 1 and 50 MeV*. Acta Radiol. Oncol. **19** 55.
- A.E. Nahum, W.H. Henry and C.K. Ross (1985) *Response of carbon- and aluminium-walled thimble chambers in ^{60}Co and 20-MeV electron beams*. Med. and Biol. Engin. and Computing, 23 Suppl part 1, p612. Proc. of VII ICMP, Espoo.
- A.E. Nahum, (1988). *Extension of the Spencer-Attix Cavity Theory to the 3-Media Situation for Electron Beams*, in “Dosimetry in Radiotherapy”, (IAEA, Vienna) Vol 1, 87 – 115.
- A.E. Nahum and M. Kristensen, (1982). *Calculated response and wall correction factors for ionization chambers exposed to ^{60}Co gamma-rays*, Med. Phys. **9** 925–927.
- A.E. Nahum, (1978). *Water/air Stopping-Power Ratios for Megavoltage Photon and Electron Beams*, Phys. Med. Biol. **23** 24–38.
- R. Nath and R.J. Schulz, (1981). *Calculated response and wall correction factors for ionization chambers exposed to ^{60}Co gamma-rays*, Med. Phys. **8** 85 –93.
- NCS 1989, *Code of Practice for the Dosimetry of High-Energy Electron Beams*. Netherlands Commission on Radiation Dosimetry, December 1989 (available from A.H.L. Aalbers, Secretary NCS, P.O. Box 1, 3720 BA Bilthoven, The Netherlands.)

- B. Nilsson, A. Montelius, P. Andreo, B. Sorcini (1988). *Perturbation Correction Factors in Ionization Chamber Dosimetry*, in “Dosimetry in Radiotherapy”, (IAEA, Vienna) Vol 1, 175 – 185.
- M.T. Niatel, A.M. Perroche-Roux and M. Boutillon, (1985). *Two determinations of W for electrons in dry-air*. Phys. Med. Biol. **30** 67 – 75.
- J.A. Rawlinson, A.F. Bielajew, P. Munro and D.M. Galbraith, (1984). *Theoretical and experimental investigation of dose enhancement due to charge storage in electron-irradiated phantoms*, Med. Phys. **11** 814 – 821.
- D.W.O. Rogers, C.K. Ross, K.R. Shortt and A.F. Bielajew, (1985a). *Comments on the ^{60}Co graphite/air stopping-power ratio used in the AAPM TG21 protocol*, Med. Phys. **13**, 964 – 966.
- D.W.O. Rogers, A.F. Bielajew and A.E. Nahum, (1985b). *Ion chamber response and wall correction factors in a ^{60}Co beam by Monte Carlo simulation*, Phys. Med. Biol. **30** 429.
- D.W.O. Rogers and A.F. Bielajew, (1986). *Differences in electron depth-dose curves calculated with EGS and ETRAN and improved energy-range relationships*, Med. Phys. **13** 687 – 694.
- D.W.O. Rogers and A.F. Bielajew (1990). *Wall Attenuation and Scatter Corrections for Ion Chambers: Measurements versus Calculations*. Phys. Med. Biol. **35** 1065 – 1078.
- D.W.O. Rogers and C.K. Ross, (1988). *The role of humidity and other correction factors in the AAPM TG-21 dosimetry protocol*, Med.Phys. **15** 40 – 48.
- R.J. Schulz, P.R. Almond, G. Kutcher, R. Loevinger, R. Nath, D.W.O. Rogers, N. Suntheralingham, K.A. Wright and F.M. Kahn, (1986). *Clarification of the AAPM Task Group 21 protocol*, Med. Phys. **13** 755 – 759.
- A. Shiragai, (1978). *A Proposal Concerning the Absorbed Dose Conversion Factor*, Phys. Med. Biol. **23** 245–252.
- A. Shiragai, (1979). *Effective Mass Stopping Power Ratio in Photon Dosimetry*, Phys. Med. Biol. **24** 452–454.
- R. M. Sternheimer and R.F. Peierls, (1971). *General expression for the density effect for the ionization loss of charged particles*, Phys. Rev. **B3**, 3681-3692.
- R. Ten Haken and B. Fraass, (1987). *Relative electron beam measurements: Scaling depths in clear polystyrene to equivalent depths in water*, Med. Phys. **14** 410 –413.
- D.I. Thwaites, (1985). *Measurements of ionization in water, polystyrene and a solid water phantom material for electron beams*, Phys. Med. Biol. **30** 41 – 53.
- M.S. Weinhaus and J.A. Meli, (1984). *Determining P_{ion} , the correction factor for recombination losses in an ionization chamber*, Med. Phys. **11** 846.
- A.Wu, A.M. Kalend, R.D. Zwicker and E.S. Sternick, (1984). *Comments on the method of energy determination for electron beams in the TG-21 protocol*, Med. Phys. **11** 871 – 874.